International Journal of Climatology

ASSESSMENTS OF MOISTURE FLUXES EAST OF THE ANDES IN SOUTH AMERICA IN A GLOBAL WARMING SCENARIO

Journal:	*International Journal of Climatology*
Manuscript ID:	JOC-07-0326.R1
Wiley - Manuscript type:	Research Article
Date Submitted by the Author:	n/a
Complete List of Authors:	Soares, Wagner; INPE, CPTEC Marengo, Jose; INPE, CPTEC
Keywords:	Low-Level Jet, Climate Change, moisture flux

ASSESSMENTS OF MOISTURE FLUXES EAST OF THE ANDES IN SOUTH AMERICA IN A GLOBAL WARMING SCENARIO

Wagner Rodrigues Soares[a,*] and Jose Antonio Marengo[a]

[a]Center for Weather Forecasts and Climate Studies (CPTEC/INPE) São Paulo, Brazil

ABSTRACT

The HadRM3P regional model from the UK Hadley Centre has been used to assess the moisture flux and the low-level jet east of the Andes in South America over two time periods: the first one can be understood as the current climate and covers the period from 1980 to 1989, and the second one covers the period from 2080 to 2089 under a future global-warming climate as projected by the IPCC SRES A2 high emission scenario. The results are analyzed considering the vertically integrated moisture transport in the lower atmosphere and the moisture flux between two core areas of South America: the Amazon Basin and the La Plata River Basins. In order to analyze the moisture transport east of the Andes, composites of South American Low-Level Jet (LLJ) were built based on wind speed and vertical wind shear following the modified Bonner Criteria 1 used to define LLJs. Integrations along the lateral boundaries of the two basins show that there could be a more intense moisture transport from tropical regions available to feed the mesoscale convective systems in the subtropical La Plata basin in the IPCC A2 scenario, as compared to the present. This is because of the intense flow to the south associated with a faster low-level jet bringing more moisture from the Amazon basin southwards. It was also observed that the presence of the low-level jet affects moisture convergence in the Amazon basin in the current climate as well as in the warmer climate. In the future high-emission scenario A2, a more intense low-level jet in a global warming climate suggests increased moisture transport from north to south east of the Andes, as compared to the present.

1. INTRODUCTION

* Mail to Wagner Rodrigues Soares, Center for Weather Forecast and Climate Studies, Rod. Presidente Durtra, km40, 12630-000 Cachoeira Paulista/SP, Brazil; e-mail wsoares@cptec.inpe.br

In several regions of the globe, strong meridional fluxes are observed in the lower atmosphere along the mountain ranges. Such events have a maximum in wind speed in the lower levels of the atmosphere (below 2000m) and are known as low-level jets LLJ (Paegle 1998). LLJ events occur on the east side of elevated topography and are associated with large-scale circulations extending over large areas, such as the Rocky Mountains in the USA (Bonner, 1968; Whiteman et al. 1997; Douglas et al. 1998) and the Andes in South America (SA) (Douglas et al. 1998; Berbery and Collini 2000; Paegle et al. 2002; Marengo et al. 2004; Vera et al. 2006a; Saulo et al. 2007 among others). Jets are also observed westward of topography, though these might not be important to transport moisture.

The studies by Bonner and Paegle (1970), as well as Paegle (1998) and Marengo et al. (2004) suggest similarities between the Rocky Mountains and the Cordillera of Andes and their effects on the occurrence of the jet. These mountains extend from tropical regions to high latitudes, blocking the zonal circulation in lower levels, and leading to the channeling of the wind. For instance, the moisture from the Gulf of Mexico in North America and northern tropical Atlantic-Amazon is transported by the LLJ to the central regions of their continents, to the Mississippi and Amazon river basins, respectively (Berbery and Collini 2000).

In South America, the LLJ is known as the South American low-level Jet SALLJ (Saulo et al. 2000, Marengo et al. 2004). The SALLJ is a component of the South America Monsoon system and transports moisture from the Amazon basin to the La Plata basin, affecting the weather and the climate east of the Andes and at the exit region of the jet in southern Brazil-northern Argentina (Vera et al. 2006a, c, Marengo et al. 2004). Thus, occurrences of the SALLJ can, through the intense moisture flow and

associated strong convective clouds in the exit region of the jet, generate rainfall extremes that produce floods (Paegle, 1998; Marengo et al. 2004, Liebmann et al. 2004).

The circulation patterns of the SALLJ can be summarized as follows: moisture is brought from the tropical Atlantic into the Amazon basin by the trade winds. Once they flow over Amazonia the air masses can gain more moisture through the intense evapotranspiration of the forest. After that, the trade winds experience a shift in direction due to the topographic blocking by the Andes and then flow parallel to the Andes towards south/southeast South America (southern Brazil and northern Argentina). Marengo et al. (2004) show that this transport exhibits an annual cycle, where in summer the moisture that goes into the La Plata basin is mostly from the Amazon region. In winter, on the other hand, even though we can have moisture transport from the Amazon region, it is observed that moisture transport of oceanic origin associated with the annual cycle of the South Atlantic Subtropical High (SASH) is stronger and dominates the annual cycle of the SALLJ.

The Amazon region contains the largest rainforest on the planet, with an area of about 7 million km^2. This basin and tropical forest ecosystem play an important role in the global energy, water and carbon balances. The La Plata basin represents a region of great economic importance in SA. This region includes the southern Brazilian states of Paraná, Santa Catarina and Rio Grande do Sul, plus Uruguay and northern Argentina. Economic activities developed in this basin, including agriculture and the generation of hydroelectric power, are sensitive to the variability of the weather and climate, becoming vulnerable to impacts related to the intense moisture transported by the jet and subsequent intense rainfall events.

Several studies based on a few isolated upper-air observations (Douglas et al. 1998; Marengo et al. 2004; Misra et al. 2000; Marengo and Soares 2002; Nicolini and Saulo

2006 and Liebmann et al. 2004) or modeling (Paegle 1998; Berri and Inzunza 1993; Nogues-Paegle and Mo 1997; Saulo et al. 2000; Herdies et al. 2002; Vernekar et al. 2003) have documented the SALLJ and the moisture transport over SA in current climate. However, there are not many studies about the of impact global warming and climate change on the variability and characteristics of the SALLJ, and on the concentration of moisture in the lower atmosphere.

Since 1988, the Intergovernmental Panel on Climate Change (IPCC) has been assessing climate change under different scenarios of greenhouse gas emissions, and also analyzing the scientific basis of climate change, impact, vulnerability and mitigation. The IPCC considers the scientific basis for climate projections into the future, and documents and quantifies its results, taking uncertainties into account. The issue of changes in the intensity of the South American monsoon system under global warming scenarios is something relatively new, and is being considered in this study. The main question is: What would be the impact of global warming upon the moisture transport from the Amazon to the La Plata basin and how would the SALLJ behave in the future?

Analysis of models from the Coupled Model Intercomparison Project (CMIP3) which contributed to the assessment of future climate change scenarios in South America in the IPCC AR4 (Vera et al. 2006b, Li et al. 2006, Christensen et al. 2007a, Meehl et al. 2007 and references quoted therein) have produced climate projections for the future, using the IPCC AR4 global models (Vera et al. 2006b; Li et al. 2006; Meelh et al. 2007 and references quoted), The models used to evaluate future climate changes have therefore evolved over time. Global models have allowed for a better scientific understanding of anthropogenic global climate change, and this has led to developments of commensurate mitigation strategies. However, at the regional scale

there remains an urgent need for relevant, targeted projections of regional climate change. Climate projections have been derived from regional models for South America (Marengo and Ambrizzi 2006, Marengo et al. 2008, Ambrizzi et. al 2007, Alves 2007). Such studies analyze changes in the temperature and rainfall as well as extreme climate events for the end of the XXI century from the scenarios of low and high emissions of greenhouse gases A2, and B2 of IPCC, respectively.

However, those studies do not analyze the behavior of the meridional moisture transport on the east side of the Andes in SA, associated with possible changes in the SALLJ activity. Marengo et al. (2007), using dynamic downscaling, showed an increase in the frequency of extreme events of rain in the far western end of the Amazon and in the south of Brazil. It is possible that this is a consequence of a future change in the regime of the transients, probably associated with cold fronts from the south or more frequent and/or intense SALLJs in a warmer climate.

The use of the dynamic downscaling technique in the generation of scenarios of the future climate makes for a better understanding of the variability typical of phenomena such as the SALLJ. Its high resolution can better present the mechanisms of surface and local factors (vegetation and topography) that affect the regional climate. Dynamic downscaling can contribute by providing details of the simulated patterns that are not obvious from global models, and this favors the investigation of moisture transport patterns in the low levels of the atmosphere, when considering projections for possible future climate of global warming.

In this paper we focus on quantification, for the present and future climate, of the moisture flux and horizontal moisture convergence over two regions, the Amazon and La Plata basins on seasonal and annual levels, focusing on the average behavior during the present climate and at the climate at the end of the XXI century. To this end,

we use two long-term simulations of 10 years each. The first one includes the period from 1980 to 1989 ("present climate") and the second one covers the period from 2080 to 2089 ("future climate"). The future climate is for the IPCC SRES scenarios (Special Report on Emissions Scenarios, Nakicenovic et al. 2000) A2 (High emission), using the HadRM3P regional model, which was run in the PRECIS system -Providing Regional Climates for Impacts Studies (Jones et al. 2004).

The analyses presented have generated an opportunity to check the behavior of the PRECIS system in simulating SALLJ events in the moisture transport associated with the jet in warmer future climates. However, the applicability and usefulness of PRECIS scenarios presented here is more for a later time slice (2080-89), and constitutes a limitation of this study, since we cannot provide discussions of climate risk information for near-term time horizons.

2. DATA AND METHODS

2.1 Characteristics of the regional model

PRECIS is a regional climate modeling system developed by the UK Hadley Centre allowing the regional model HadRM3P, to be run over any area of the globe (see Jones et al. 2004, which also includes a detailed description of HadRM3P). There are 19 vertical levels and two horizontal resolutions to pick from in HadRM3P. In this study, a 50-km horizontal resolution and 1-day temporal resolution was used. Lateral boundary conditions for HadRM3P are available from a range of model- and observationally-based sources. In this study they are obtained from the global atmospheric, HadAM3P. The horizontal resolution of HadAM3P is 1.25° latitude by 1.875° longitude and the model formulation is the same as HadRM3P.

As suggested in the PRECIS technical manual, the simulations were initiated in December of 1979 and December of 2079 and run until the end of 1989 and 2089, respectively. The extra integration time was assumed to be sufficient to allow for model "spin-up", which should be a few days for the atmosphere, although for soil processes (moisture) it could take a few seasons (Giorgi and Mearns 1999), or even a few years (Robock et al. 1998).

Rowell (2005) described and synthesized the experimental design of the driving HadAM3P experiment as follows. The HadAM3P 1980-89 simulation is forced by observed sea-surface temperatures and sea-ice (SSTs) from the HadISST1 dataset (Rayner et al. 2003). For the future period, 2080-89, HadAM3P is forced by SSTs which are formed from observed SSTs altered by the sum of mean changes and trends calculated from a global coupled model projection. The coupled integration was performed with HadCM3 (Gordon et al. 2000) whose atmospheric component, HadAM3 (Pope et al. 1999), is the basis for HadAM3P (Jones et al. 2007). The same SSTs were used as the lower boundary condition for the HadRM3P simulations.

The domain utilized (shaded grey in Fig. 1) appears to be sufficiently large so that the regional model can develop its own internal circulation on a regional scale, but not so large that the climate of the HadRM3P would depart significantly from the global model in the center of the domain (Giorgi and Mearns 1999; Chou et al. 2005).

2.2. Simulations using HadRM3P and characteristics of the IPCC warming scenario

For this study, two long-term simulations were performed using HadRM3P with a spatial resolution of 50 Km (lat/lon) and a time step of 1 day from which the climate projections were obtained for the two 10-year periods. The first simulation covers the

period from 1980 to 1989 and can be considered as current climate. The second simulation embraces the period from 2080-89 and represents a possible future climate from the IPCC SRES A2 scenario. The CO2 concentration in the SRES A2 is about ~300ppm during the 1980's and about ~700ppm during 2080's. The NO_2 concentrations are about 280 and 400 ppb and the CH4 concentrations are from 1500 and 3200 ppb during the decades of 1980 and 2080, respectively (IPCC, 2007 a, b).

For the proposed assessments of moisture transport and moisture convergence at lower levels, mean flow and SALLJ composites for present climate have been prepared for the 1980-89 present-climate simulations from the HadRM3P. Before that, validations of the simulated present climate are done using the NCEP-NCAR reanalyses (Kalnay et al. 1996). Simulated present precipitation was compared with CRU (Climatic Research Unit - www.cru.uea.ac.uk) gridded data.

2.3. Detection of low-level jet events

To detect and characterize SALLJ events, the modified Bonner criteria 1 (Bonner, 1968) were used. These modified criteria specify that the magnitude of the wind has to be equal to or larger than 12 m s^{-1} on the 850 hPa level, the vertical wind shear has to be at least 6 m s^{-1} between the 850-700 hPa levels and the meridional component of the wind has to be negative and larger in magnitude than the zonal component. These modified criteria were applied for the daily data at a grid point in Santa Cruz de la Sierra (16.7S, 63W) in Bolivia, a location that represents the main axis of the jet, as in previous studies (Douglas et al. 1998, Saulo et al. 2000, Nicolini et al. 2002, Salio et al. 2002, Marengo et al. 2004 and Saulo et al. 2007 among others). Later

on, composites of SALLJ episodes were assembled by grouping SALLJ events in each season of the year, for the future and present climate.

2.4. Definition of the area of study

The La Plata basin is influenced by the annual cycle of moisture in the lower levels of the atmosphere, mainly from the tropical region of SA. The Amazon forest is one of the sources of moisture for regions in the south of Brazil such as the La Plata basin region (SALLJ exit region), particularly during spring and summer. Other moisture sources for this region are: moisture associated with the presence of the SASH, and the sea breeze, mainly during fall and winter.

With the objective of quantifying the moisture flux between the Amazon and the La Plata basins, two areas were chosen whose lateral borders are shown in Figure 1.

The two areas chosen for the computation of horizontal moisture divergence were: A (Amazon basin) lat=10°S, 0°; lon=65°W, 45°W, and P (La Plata basin) lat=25°S, 35°S; lon=65°W, 45°W. The lateral borders of those areas were established as: north of the Amazon basin (NA), lat= 0°; lon= 65°W, 45°W, south of the Amazon basin (SA), lat= 10°S; lon= 65°W, 45°W, east of the Amazon basin (EA), lon=45°W; lat=0°,10°S, west of the Amazon basin (WA), lon=65°W; lat=0°,10°S, north of the La Plata basin (NP), lat=25°S; lon=65°W, 45°W, south of the La Plata basin (SP), lat=35°S; lon=65°W, 45°W, east of the La Plata basin (EP), lon= 45°W; lat=25°S, 35°S, west of the La Plata basin (WP), lon=65°W; lat=25°S,35°S.

2.5. Quantification of the moisture flux and horizontal moisture divergence

The vertically integrated moisture flux was calculated from the following equations:

$$Q_v = \frac{1}{g}\int_{pt}^{po} qv\, dp \quad (1)$$

$$Q_u = \frac{1}{g}\int_{pt}^{po} qu\, dp \quad (2)$$

Where Q_v is the meridional moisture flux, Q_u is the zonal moisture flux, g is gravity, q is the specific humidity, u and v are the zonal and meridional components of the wind, and pt and po represent the pressure at 700hPa and the surface, respectively (Rao et al. 1999).

The moisture flux along the lateral borders was calculated from the following equations:

$$Q_j = \int_{la1}^{lao} Q_i\, dy \quad (3)$$

$$Q_k = \int_{lo1}^{loo} Q_i\, dx \quad (4)$$

In equations 3 and 4, the integration is made by fixing the latitude or longitude along the borders. The index j defines the longitude of the eastern or western borders (integration towards y), l_{a1} is the latitude of the southern border and l_{a0} and the latitude of the northern border. The index i defines the meridional or zonal moisture flux already vertically integrated. The index k (integration towards x) fixes the latitude to define the northern or southern borders. l_{o1} is the longitude of the western border and l_{o0} is the longitude of the eastern border.

The horizontal moisture divergence was obtained from Q_v and $Q_{u,}$ which provided the vertically integrated zonal and meridional moisture fluxes. The calculation was made at each grid point using finite differences. The results are shown for four seasons: DJF (December-January-February), MAM (March-April-May), JJA (June-

July-August), and SON (September-October-November). In the results, negative values of divergence mean convergence.

3. RESULTS AND DISCUSSION

3.1. Validation of the regional model in the low levels of the atmosphere for the current climate

The moisture flux as well as the horizontal moisture divergence fields was derived from the specific humidity and components of the wind from surface to 700 hPa. For validation purposes, the specific humidity and zonal and meridional components of the wind generated from the regional model HadRM3P were compared to those derived from the NCEP-NCAR reanalysis.

Figure 2 shows the water vapor fields below 700 hPa. Figure 2a represents the mean field for the period from 1980 to 1989 for the months DJF, and Figure 2b represents the same field and period from the HadRM3P simulations. Comparison of the figures, shows a pattern of similarities in the spatial distribution and the values. Specific humidity varies from 3 to 9 g kg^{-1} in both NCEP-NCAR and HadRM3P over South America., except in an area close to the Andes, where the reanalyses show higher values. Figure 2c (difference between Figures 2b and 2a) shows a difference over the continent of less than 1 g kg^{-1}, while over the Andes, this difference reaches 3 g kg^{-1}. Over the northeast region the regional model shows moisture values lower than those of NCEP-NCAR by around 1 g kg^{-1}. In the north of Argentina and south/southeast of Brazil, the regional model shows areas with specific humidity derived from NCEP-NCAR reanalyses around 1 g kg^{-1} larger than the regional model during austral fall (MAM), there is a similarity between the simulations and the NCEP-NCAR reanalyses

in the distribution and values of specific humidity, which was also observed during austral summer, DJF. The regional model projections show larger moisture values (by about 2 g kg^{-1}) over northern Argentina and Paraguay as compared to the NCEP-NCAR reanalyses, while over a region between 10 and 24°S and 45°W (Figure 2f), the model shows values lower than those in the reanalyses. During austral winter (JJA), Figure 2i shows that for the region between 10°N and 2°N, the regional model presents large specific humidity values--about ~ 1 - 2 g kg^{-1} greater than those in the NCEP-NCAR reanalyses. Figures 2g and 2h show large values of humidity in the northeastern region of South America as depicted by the model, while the reanalyses show large values in the Northwest, with values over the continent of about 9-12 g kg^{-1}. In austral spring (SON) the regional model depicts lower humidity values in Northeast Brazil as compared to the reanalyses, by about 2 g kg^{-1}, while over regions such as northern Paraguay, western Amazonia and the Atlantic Ocean off the coast of Northeast Brazil the difference is smaller (~ 1 g kg^{-1}). In general, we can affirm that the regional model shows mean specific humidity values that are of the same order of magnitude as those from the reanalyses, with similar spatial distribution and with some systematic positive or negative biases in some regions. The differences may be due also to the differing resolutions of the regional model and the reanalyses.

The zonal component of the mean wind below 700 hPa during DJF in Figs 3a and 3b shows the intense northeast trade winds in both the NCEP-NCAR reanalyses and the regional model output. On the east side of Andes, a center of intense zonal wind of about 3 m s^{-1} has been detected to the east of Bolivia. The zonal wind difference between the regional model and the reanalyses (Figure 3c), shows positive values in northern Amazonia, suggesting that the regional model is underestimating the zonal

wind intensity from the reanalyses, by about 3 m s^{-1}. In northeastern Brazil, between 10S and 45W there is an overestimate of the zonal winds by the regional model as compared to the reanalyses in austral summer. In the fall (MAM), Figures 3d and 3e indicate that both the regional model and reanalyses show the trade winds, but to the east of the Andes the regional model shows a less intense flow as compared to the reanalyses, by about 3 m s^{-1}. The difference map (Figure 3F), shows the underestimation of the zonal wind in the tropical region both over the continent and the tropical Atlantic Ocean by the regional model. By comparing Figures 3g and 3h it is seen that the regional model shows more intense zonal wind flow around 20S and 55W. In winter (JJA), the regional model underestimates the zonal wind in an area from the northeast trade winds over northern Amazonia reaching into Bolivia. More intense values are observed in the region of SASH in the regional model (Figure 3i). In the months SON, as well as in other seasons of the year, the mean zonal flow is similar in the regional model (Figure 3k) to that in the NCEP-NCAR reanalysis (Figure 3J), and the difference maps (Figure 3l) show smaller values in winter than in other periods of the year. While an underestimate has been noticed over Amazonia, an overestimate has been detected in the south/southeast of Brazil.

The meridional component of the wind during DJF (Figures 4a and b) shows that the regional model depicts the northerly flow over the Amazon and the east side of the Andes, and the HadRM3P simulates a more intense northward flow as compared to the reanalyses. The difference maps (Figure 4c) show an overestimation of the meridional flow as compared to the NCEP-NCAR reanalyses over central Brazil. This may be due to the better depiction of the topography. During MAM, the decrease in the intensity of the meridional component of the wind is noticed in both the regional model and the

reanalyses (Figures 4d and e). The difference map (Figure 4F) exhibits smaller differences next to the coast of Brazil and larger differences over Central Brazil and northern Argentina. During winter (JJA), the circulation patterns are similar in the regional model (Figure 4h) and the NCEP-NCAR reanalyses (Figure 4g). The largest differences are observed over northern Argentina, where the regional model overestimates the intense meridional northerly flow from the reanalyses (Figure 4i). Figures 4j and 4k, show an intense northerly flow over Bolivia during spring (SON), which the regional model carries to a position more to the south than does the reanalysis. The difference map (Figure 4l) shows a stronger meridional wind in the regional model on the southern coast of Brazil, suggesting that in this region the circulation associated with SASH is more intense in the regional model than in the reanalyses.

3.2. Variability and characteristics of the SALLJ in the current and future climate using regional modeling

Figure 5 shows the number of SALLJ events detected at Santa Cruz de la Sierra (17.7S, 63W), using the modified Bonner criteria 1 specified in item 2.3, for both present and future climate. It is observed that in the current climate the SALLJ annual cycle in the present is similar to that simulated in the global warming scenario for the end of the XXI century.

A comparison among the simulated cases in the present and in the future shows that during DJF, the number of LLJs detected goes from 45 for the present to 78 in the A2 scenario. This is an increase of about 73% in the occurrence of SALLJs in the climate of warming in SRES A2. On the other hand, during MAM the number of LLJs

detected is very close, 37 cases in the current climate versus 43 in the A2 scenario (an increase of about 16%). In JJA, the number of SALLJs varies from 62 in the present to 88 in the A2 scenario, which is equivalent to an increase of 41%. In SON more LLJs were detected in the future climate than in the present. The number decreases from 25 to 15, that is, during this period the number of LLJs is about 60% smaller in the SRES A2 from 2080 to 2089 as compared to the present. This decrease of the number of SALLJs may be associated with the decrease of the vertical wind shear in this period, and would suggest a vertical stretching of the jet axis.

The total number of cases of detected jets using the HadRM3P model simulations was 169 between 1980 and 1989, and 224 between 2080 and 2089. The 55 additional cases of SALLJ events detected in the global warming climate can be considered an indicator of an intensification of the regional circulation and the SALLJs, with the jets more frequent and possibly faster than in the present, especially during summer and spring. This would have impacts in the regimes of extreme rainfall events at the exit region in the La Plata region, and in fact the number of intense rainfall events in southern and southeastern Brazil has increased during the last years (Marengo et al. 2007). It is important to mention that for the present climate 1980-89, the modified Bonner criteria 1 were applied to the four seasons in the NCEP-NCAR reanalysis circulation fields. The results indicate that 28 cases of SALLJ were obtained during DJF, 18 for MAM, 5 for JJA and 9 for SON with a total of 60 detected jets from 1980 to 1989, as compared to 169 simulated for the HadRM3P model during 1980-89. This indicates that the model tends to overestimate the number of SALLJ events in the present, and the different resolutions of the regional model and the reanalyses could be the main cause. However, based on the model results only, an increase of 25% in the

number of SALLJ events is noticed in the warmer climate, especially in summer, where the increase reaches 72%.

Figures 6 a and b show the wind speed at the 850 hPa level, as well as values of the vertical wind shear between the 850 and 700 hPa levels. Figure 6 shows an overestimate of the wind and of the vertical shear in relation to the NCEP-NCAR reanalyses. This overestimate could be due mainly to the diffence in resolution between the regional model and the reanalyses.

In relation to the magnitude of the mean wind field, a seasonal variability with higher values can be observed during JJA and lower values during MAM for both current climate and the future climate in the SRES A2 scenario. In present and future climate, the average of vertical wind shear has values lower than 3m s^{-1}.

In Figure 6b, for the SALLJ composite, after the application of the modified Bonner criteria, an increment is observed in the wind speed and vertical wind shear as compared to the climatology. The values of the horizontal wind over Santa Cruz de la Sierra can be higher than 20m s^{-1} during JJA. It is also observed that the vertical wind shear in the SALLJ composite reaches values of about 8m s^{-1} (Figure 6b). This shows that the regional model used in this study detected cases of SALLJ which satisfy even the modified Bonner criteria 1, as in the SALLJ event that occurred during December 2003 in the the SALLJEX field experiment (Vera et al. 2006c) and was studied by Saulo et al. (2007).

Figure 6 shows an intensification of the wind speed observed in the global warming climate. The increase of the jet speed in the future scenario can be associated with an intensification of the thermal gradient between tropical and subtropical South America, as shown by Ambrizzi et al. (2007) and Marengo et al. (2007). There are indications that the thermal Chaco low would be intensified in a warmer climate, and

this would increase the meridional pressure gradient, increasing the intensity of the SALLJ.

Uccellini and Johnson (1979) related the presence of the high-level jets to the formation of LLJs east of the mountains. In a warming climate, the more intense SALLJ activity could be also associated, through the adjustment of mass, with the intensification of the maximum speed of the upper-level subtropical jet.

3.3. Meridional moisture transport associated with the SALLJ

Figure 7 shows a vertical cross section of the meridional moisture transport fields for the SALLJ composite along the latitude of Santa Cruz de la Sierra (17.7S). From summer to fall, a larger meridional moisture transport is detected mainly in the core of the SALLJ (~63W) in the global warming high-emission scenario A2, as compared to the current climate. The set of panels from Figure 7 shows that in relation to the vertical structure of the meridional moisture transport, in the global warming scenario moisture transport is intensified towards the east as well as with height. In the global warming climate, the meridional moisture transport can be higher by 60 m g s^{-1} kg^{-1} next to the Andes as compared to the present. Furthermore, in addition to the core region of strong northerly moisture transport of the SALLJ during DJF and SON, a secondary nucleus is observed, linked to the moisture transport from the South Atlantic Ocean, with a large northerly meridional moisture transport located between 40 and 55W in the current climate as well as in the global warming scenario.

For present climates, Saulo et al. (2000), Nicolini et al. (2002) and Marengo et al. (2004) have detected this secondary nucleus as corresponding to the northerly flow associated with the SASH, whose moisture transport is more intense during winter. Also, the SASH is stronger and closer to the continent during that season, and the

elevated topography in this "Planalto" region would also have a channeling effect on the wind. The more intense meridional moisture transport is detected at about 63W, and is larger (about 30 m g s^{-1} kg^{-1}) in the warming scenario. This can be explained by examining Figure 8, which shows the characteristics of each component of this moisture transport along the Santa Cruz de La Sierra latitude.

Figure 8 shows that the regional model positions the core of the SALLJ between 60 and 63W, a location very similar to that shown by Marengo et al. 2004, who used 50 years of NCEP-NCAR data in his study of this jet. Moreover, the values of northerly wind components of around 10-12 m s^{-1} and of specific humidity that vary between 15 and 21 g kg^{-1}, in the lower atmosphere, are quite close to those shown by Marengo et al. 2004 who utilized data from the NCEP-NCAR reanalyses.

In the global warming scenario, for the period of DJF (Figure 8e) there appears to be a higher moisture content from the surface to 700hPa between 60 and 45W, as compared to the present (Figure 8a), while the intensity of the meridional component of the wind in the lower levels of the atmosphere is weaker. This is emphasized by Figure 6b, which shows wind speeds smaller than 1 m s^{-1} at 850 hPa over Santa Cruz de La Sierra. So, the intense moisture transport that is revealed in the gobal warming scenario is due the intensification of the moisture content rather than to the intensification of the winds.

During MAM, a higher moisture content concentrated near the Andes is detected in the global warming scenario (Figure 8f) as compared to the current climate (Figure 8b). Also, the wind is stronger (see Figure 6b) and with a larger contribution to the meridional moisture transport (Figure 7F compared to Figure 7b).

For JJA, Figure 8c and 9g show the patterns of wind and moisture simulated for the present and projected for the future, respectively. The fields show similarity to those

of DJF in terms of the magnitude of the moisture content and wind intensity, with the exception of a nucleus of higher moisture content during JJA. On the other hand, for SON, Figure 8h shows that there is a larger contribution of the wind speed (meridional component) as compared to the contribution of moisture content in the global warming scenario. When compared to present climate (Figure 8d), Figure 8h shows a nucleus of meridional flow more intense to the east of the Andes, which can also be seen in Figure 6b. Besides the wind, the moisture content in the lower levels of the atmosphere also contributes to the higher meridional moisture transport in the global warming climate when compared to the present (Figure 7h compared to Figure 7d).

A nucleus of large moisture content is observed in lower levels around 850 hPa in the global warming scenario (Figure 8h) as compared to the present climate (Figure 8d). This increase in the moisture content in the global warming climate scenario extends from the lower levels to ~700hPa and is able to affect the moisture that moves from tropical regions east of the Andes to the La Plata basin. This is discussed in the next section.

Therefore, it could be suggested that the higher moisture transport carried out by the SALLJ in a global warming scenario (set of Figures 7) might be due to the higher wind speed and the large moisture content in the lower levels of the atmosphere. It is important to highlight that the large wind speed at the low levels of the atmosphere in the global warming scenarios has been detected in all seasons but there are differences in the intensity of the wind in the annual cycle, as shown in Figures 6 and 8. The large amounts of moisture in the lower levels of the atmosphere detected in the global warming scenario as compared to the present climate may affect the magnitude and the seasonal variability of the meridional moisture transport. The DJF season is an example of a situation in which the moisture content at the lower levels east of the Andes seems

to contribute more than the wind speed to moisture transport, as shown in Figure 8e (warming scenario) versus Figure 8a (present climate). This is not so evident in MAM (Figure 9f versus Figure 9b) where the meridional component of the wind seems to have a more important role than the moisture content. The intensification of the meridional moisture transport shown here can have an effect on the moisture fluxes from the Amazon into the La Plata basin.

3.4. Vertically integrated moisture transport

Figure 9 shows the vertically integrated moisture transport fields between surface and 700 hPa. The patterns simulated by the HadRM3P for summer and winter during 1980-89 are consistent with the ones presented by Nicolini et al. (2002), Marengo et al. (2004) and Salio et al. (2007), who used data from the NCEP-NCAR and ECMWF reanalyses. Besides the intense transport next to the equator associated with the trade winds, the model simulates the shifting of the wind direction when the trades encounter the Andes and afterwords when the winds are deflected southeast, towards the La Plata basin. The influence of SASH in the moisture transport is also represented by the regional model, as shown in Figure 9.

The seasonal analyses during 1980-1989 (Figures 9a to 9d) show that the zonal component of the moisture transport, associated with the northeast trade winds is more intense in the region of the tropical Atlantic ocean (between 0 and ~10S) than over the Amazon region. During DJF and SON, close to the north/northeast part of the Brazilian coast, the flow is more zonal while in MAM and JJA a strong southward flow is observed due to the action of SASH, which is more active and closer to the continent at this time of the year. In the period from 2080 to 2089, the northeast trades are active over northern and northeastern Brazil. An intensification of the moisture transport as

compared to 1980-89 is detected over the coast of northeastern Brazil and on the eastern side of the Andes. The latter is possibly due to the deepening of the Chaco Low in the global warming scenario, as shown by Vera et al. (2006c), and as shown in Figures. 9e to 9h.

In general in the global warming scenario climate over South America, the moisture transport in the lower levels of the atmosphere is intensified along the eastern side of the Andes. An intensification of the trade winds is detected in all seasons in the future. In addition, the meridional moisture transport can be higher in the global warming scenario. Further south, moisture transport along the eastern side of the Andes also becomes more intense, which is attributed to the mechanisms described in section 3.2 and the components of meridional moisture transport, as discussed in section 3.3.

In both the present and global warming climate scenarios, the presence of the SALLJ, as expected, suggests an increase in the moisture transport along the eastern side of the Andes (Figures 9i to 9p). This may increase the moisture convergence at the exit region of the SALLJ and consequently, favor an increase in convection and the occurrence of extreme events of precipitation in southern Brazil, as suggested by Saulo et al. (2007) and Marengo et al. (2007). In addition to an increase in the moisture convergence, a possible increase of cold front penetrations from the south in a global warming scenario can also contribute to an increase in the frequency and intensity of rainfall extremes in the La Plata basin.

3.5. Mosture Flux in the lateral borders of the areas under study

In this section we make a comparison between the simulated mean integrated fluxes for the present and the future, already described in Section 2.5. The analysis is

shown in Figs. 10 to 13: Figures 10a to 10b (DJF), 11a to 11b (MAM), 12a to 12b (JJA) and 13a to 13b (SON). For summertime in the present climate Nicolini et al. (2002) used the Eta/CPTEC regional model and obtained a value of -1.9×10^{-8} kg s^{-1} for the northerly flux crossing the latitude of 20S along 45W and 64W, which represents the northern border of a box in the La Plata region. In the same latitudinal border, and also using the Eta/CPTEC regional model, Saulo et al. (2000), obtained -1.9×10^{-8}kg s^{-1} for the summer period, and -1.84×10^{-8} kg s^{-1} for spring, integrating the flows from the surface to 800hPa. These values are very close to the ones obtained by HadRM3P on the border NP from the present-climate simulation.

Our analysis is focused along the lateral borders of the boxes representative of the Amazon (A) and the La Plata basin (P). In DJF (comparison between Figs. 10a and 10b) on the NA border in SRES A2, the moisture flux is 64% greather than present climate. On the border of EA, a similar increase in moisture flow increase is observed. On the border of WA there is an increase of about 45% in the intensity of the westerly flux in the global warming scenario as compared to the present. On the border of SA the moisture flux increases by 75% in the future. During MAM (Figures 11a and b) and SON (Figures 13a and b), an intensification is also detected in the moisture flux that enters across the EA and NA borders and that leaves across the WA and SA borders in the future. In contrast, in JJA, Figure 12a (current climate) exhibits a southerly flow entering across the SA border and leaving the box across the NA border. This occurs because the meridional component of the trade winds comes from the south over the continent, as observed in Figure 9c, at a time of the year when the SASH is more intense and closer to the continent.

At the lateral borders of the La Plata basin, an intensification of the flux that penetrates across the northern border NP in the global warming scenario is detected.

During DJF there is an increase of ~50% in the lower atmosphere moisture flux in the SRES A2 global warming scenario across the NP border. In other seasons, an intensification of the northerly flux across the NP border in a global warming scenario is also observed. For MAM, the flux increases +58%, for JJA +44% and in SON it increases +72%.

In what follows we discuss the influence of the presence of the SALLJ on the moisture flux between the A and P regions. In the current climate and comparing the mean present climate and the SALLJ composites during DJF, an intensification of the moisture penetration in the region of the La Plata basin is observed on the border NP that is approximately equivalent to an increase of 60% in the northerly flux in the summer SALLJ composite as compared to the summer mean. For MAM, JJA and SON the same pattern is detected for the SALLJ composite, suggesting an intensification of the moisture flux on the NP border in the SALLJ composite. In MAM an increase of about 136% was observed. In JJA the value becomes about 120% higher. In spring (SON), the SALLJ composite shows an increase of 170% as compared to the spring mean.

The SALLJ in the current climate accelerates the moisture transport to the east of the Andes. That increases the moisture flux towards the La Plata basin, as shown in various studies. The northerly flux of -3.85×10^{-8} kg s^{-1} entering the La Plata basin at 20S, derived by Nicolini et al. (2002) compares favorably with the estimates of -3.14×10^{-8} kg s^{-1} at the same border derived from the HadRM3P at this border for 1980-89, as shown in Figure 10c.

In the global warming scenario, there is an increase in the moisture flux that crosses the northern boundary NP. During DJF, this value increase 47%. During MAM,

the increase reaches about 111%, while during JJA the increase is about 103%, and during SON, the increase reaches about 156%.

The moisture flux in the SALLJ composite in a global warming scenario shows a more intense flow from the tropical region into the northern border NP of the La Plata basin, east of the Andes (Figure 9). In the global warming scenario, Figures 10d, 11d, 12d and 13d show higher moisture flux crossing the NP border when compared to the present climate (Figures 10c, 11c, 12c and 13c). The SALLJ composite for DJF shows an increase in the moisture flux of about 40%. In MAM, this increase is about 41%. In JJA, the increase is about 33%, while in spring (SON), the moisture flux value increases by about 63%. This increase in all seasons suggest that the SALLJ is more active in the global warming climate scenario than in the current climate, transporting larger amounts of low-level moisture from the Amazon region towards the La Plata basin. It is also important to highlight that the low level circulation associated with the SASH also transports moisture to the La Plata region as shown in Figure 9. This moisture flux enters the Amazon box (A) through the WP and NP borders.

In a global warming climate, the trade winds would become more intense due to the higher thermal contrast between the ocean and the continent. Over the Amazon there would be a higher amount of moisture in the lower atmosphere transported from the tropical Atlantic. This moisture would be channeled by the Andes and transported towards the La Plata basin more efficiently by the presence of more frequent SALLJ events.

3.6. Impact of the warming scenario and presence of the SALLJ on the moisture convergence and precipitation in the Amazon and La Plata basins

In this section we perform an analysis of the effect of the presence of the SALLJ on the low-level moisture convergence and precipitation over the Amazon and La Plata basins. The convergence and precipitation values are obtained from average area in the boxes A and P shown in Figure 1.

In the Amazon basin the HadRM3P underestimates the convergence as compared to values obtained from the NCEP-NCAR data, while in the La Plata basin an overestimate of the convergence of the regional model in relation to that of NCEP-NCAR is seen.

Figure 14, which compares the values of mean convergence in the present to that of the future climate simulated by HadRM3P, shows during DJF, MAM, JJA and SON that an increase can also be observed in the moisture convergence in the Amazon in the global warming scenario. This increase in the average moisture convergence in area A, occurs mainly by the strengthening of the moisture flow associated with the trade winds (see Figure 9a and 9e), as a response to the higher differential warming (continent/ocean). In winter, as the SASH is more active and closer to the continent this also strengthens the trades and provides them with a more zonal outlet, as shown by Marengo et al. (2004).

Figure 14 show that the presence of the SALLJ in the current climate as well as in the SRES A2 global warming scenario induces a reduction of convergence in the Amazon region. Figure 10 shows that the moisture flux that comes out of the Amazon region through the WA and SP borders is quite strong in the presence of the SALLJ composite in the present climate (Figures 9i to 9l) as well as in the global warming scenario (Figures 9m to 9p).

Comparing the effect on the SALLJ for the present versus the future climate, it is shown that in the Amazon region there is an increase of the convergence in the SRES

A2 scenario. This is due to the fact that the moisture flux that enters the Amazon is intensified in the SRES A2. This intensification can be observed on the border EA when comparing the Figures 10d to 10c, 11d to 11c, 12d to 12c, and 13d to 13c at a seasonal level.

For the La Plata basin, the right side of Figure 14 shows that in the mean there is an increase of the moisture convergence in SRES A2 as compared to the average value for the present climate. This is because the flux that leaves the Amazon mainly through the SA and WA borders and that reaches the La Plata basin is more intense in the global warming scenario.

In the La Plata basin the effect of the presence of the SALLJ along the east side of the Andes, in the current climate as well as in the global warming climate, is opposite to that in the Amazon basin. This means that in the La Plata basin the moisture convergence increases in the presence of the jet precisely because the flows that penetrate this basin are intensified, as discussed in the previous session. The comparison of the SALLJ composite in the global warming scenario versus the present climate at the seasonal level suggests that there is a higher moisture convergence in the La Plata basin in SRES A2. This happens because the flow that enters the NP border is stronger.

The analyses have shown that due to the fact that the moisture flux becomes more intense in the global warming scenario, larger horizontal moisture convergence over the Amazon and La Plata basins may occur. Furthermore, the presence of SALLJ in both present and future climates suggest an increase in the moisture flux that crosses the western and southern boundaries of the Amazon, generating a decrease in the moisture convergence over the Amazon and an increase over the La Plata basin.

This apparent acceleration of the hydrological cycle can also explain the increases in the frequency of the rainfall extreme events in the south of Brasil-Uruguay-

northern Argentina, as detected by Marengo et al. (2007) for the IPCC SRES A2 scenario.

In relation to precipitation, Figure 15 shows that the regional model underestimates the data of the CRU over the Amazon region, while in the La Plata basin region, the model overestimates the precipitation. Even if the data of the CRU are considered as observations, apparently the regional model captures well not only the annual cycle of precipitation in Amazonia, but also in the La Plata basin. Normally in Amazonia, a larger quantity of rain is observed during DJF than MAM, as the HadRM3P showed.

Generally, under strong global warming, Amazonia would have a drier climate with less rain throughout the year, but here the the La Plata basin would have a larger quantity of rain. These results agree with those of Marengo et al. (2007) which showed that more extreme rain events in the southern region of Brazil in the SRES A2 scenario.

In the current climate as well as in the warming scenario, Figure 15 shows that when the SALLJ is present the Amazon region has less rain. The contrary occurs in the La Plata basin, where a larger quantity of rain is observed when SALLJ events are occurring.

Larger quantities of rain are observed in the presence of the SALLJ in the warming scenario. This can be attributed to the more intense flux of moisture associated with the jet, causing more moisture convergence in this region, as can be seen in Fig. 14. This may be in the form of extreme rainfall events.

4. CONCLUSIONS

Simulations of warmer future climates projected by the HadRM3P regional model from the UK Hadley Centre, suggest that in the IPCC SRES A2 scenario, to the east of the Andes the projections show a higher frequency of SALLJ events, as compared to the present. Besides this higher frequency, the regional model projections also suggest an increase in the speed of the SALLJ in the global warming scenario.

The SALLJ composites for the present climate cause an increase of meridional moisture transport in the lower atmosphere, mainly in an area along the eastern side of the Andes, towards southeastern South America, as many papers have suggested (Saulo et al. 2000; Nicolini et al. 2002; Marengo et al. 2004; Saulo et al. 2007 and Salio et al. 2007). In the global warming scenario, the presence of the SALLJ intensifies significantly the meridional moisture transport in this region due to an increase in the meridional temperature gradient between tropical and subtropical South America east of the Andes.

The largest moisture transport that happens in the presence of SALLJ in a global warming scenario climate is due to a higher wind speed and moisture content in the lower level of the atmosphere, although there are differences in the intensity of the annual cycle of the wind, and higher wind speed in the lower levels of the atmosphere has been detected in the global warming scenario throughout the year.

The comparison of the SALLJ composites for the present and future has shown an increase of the moisture flow across all the lateral boundaries of the Amazon and La Plata basins. Thus, in a global warming scenario, mainly in the La Plata basin, due to the maximum in moisture convergence, this could imply higher moisture amounts available to feed the convective mesoscale systems which form in this region, and possibly increase the frequency of the rainfall extremes.

On the other hand, the results presented here have shown that the presence of the jet has caused a decrease of the moisture convergence in the Amazon in the current climate as well as in the global warming climate, suggesting less rainfall during SALLJ events, mainly in central and eastern Amazonia. In the present climate, less intense moisture fluxes were detected in the subtropical Atlantic Ocean in the presence of SALLJ.

The average flow east of the Andes in SRES A2 is higher than in the period from 1980 to 1989 and becomes even higher in the presence of the SALLJ. This suggests that the SALLJ transports moisture more efficiently in the global warming scenario SRES A2, and this could imply an increase of the precipitation in this region, especially in the form of frequent extreme rain events.

The integration of the moisture flux along the lateral boundaries of the Amazon and La Plata boxes has shown that in the global warming climate in the Amazon region, the average moisture flux is more intense. Therefore, the presence of the SALLJ in both the present climate and the future SRES A2 warm climate has caused an increase of the moisture flux which crosses the west and/or south boundaries of the Amazon, causing a decrease of the moisture horizontal convergence there and an increase in the region of the La Plata basin. A higher moisture concentration may be available to be transported by SALLJ down to the southeastern region of South America. Thus, SALLJ can work as a modulator of the hydrological cycle between the two regions, and lead to an even higher convection and possibly more extreme events of rain in the south/southeast region of South America in a global warming scenario. Therefore, the annual cycle has shown a higher amount of moisture from the tropical Atlantic transported by the intensified trade winds, due to a warmer climate, and this allows for a higher amount of moisture in the lower atmosphere that is transported by the SALLJ.

We want to emphasize that the simulations presented in this paper do not consider changes in the vegetation, such as the deforestation of the Amazon, and also the "Amazon die-back" effect (Cox et al. 2000) which could, in a global warming scenario caused by higher concentration of greenhouse gases, have opposite impacts on the hydrological cycle over South America. Correia et al. (2007), Sampaio et al. (2007), and Salazar et al. (2007) showed in their studies of the deforestation effects in the Amazon that the region is becoming drier. Thus, in a scenario of strong warming like SRES A2, a higher moisture transport from the north associated with the SALLJ is detected. Deforestation would lead to a weakening of such transport since there would be a smaller amount of moisture in the lower atmosphere available to be transported by SALLJ to the south/southeast region of South America.

AKNOWLEDGEMENTS

The authors thank the Foundation of Support for Research of São Paulo State (FAPESP - Reference N°. 02/12670-6), the UK GOF-Dangerous Climate Change project, PROBIO, GEOMA and LBA Instituto do Milenio II projects for the financial support for the development of this article. We also thank especially the Hadley Centre for Climate Research and Prediction UK for enabling the use of the PRECIS modeling system and data for the simulations of future climates.

REFERENCES

Alves L. 2007. Simulações da variabilidade do clima presente sobre a América do Sul utilizando um modelo climático regional. *Master Science Dissertation*, INPE. São José dos Campos, Brazil.

Ambrizzi T, Rocha R, Marengo J, Pisnitchenko AI, Alves L, Fernandez JP. 2007. Cenários regionalizados de clima no Brasil para o século XXI: projeções de clima usando três modelos regionais". *Relatório 3*, Ministério do Meio Ambiente , Secretaria de Biodiversidade e Florestas, Diretoria de Conservação da Biodiversidade

- Mudanças climáticas globais e efeitos sobre a biodiversidade – Sub projeto: Caracterização do clima atual e definição das alterações climáticas para o território brasileiro ao longo do século XXI. Brasilia, 108 .

Berbery HE, Collini E. 2000. Springtime precipitation and water vapor flux over southeastern South American. *Montly Weather Review* **128**: 1328-1346.

Berri GJ, Inzunza B. 1993. The Effect of the Low-Level Jet on the Poleward Water Vapor Transport in the Central Region of South America. *Atmospheric Environment* **27A**: 335-341.

Betts R, Cox P, Collins M, Harris P, Huntingford C, Jones P. 2004. The role of ecosystem-atmosphere interactions in simulated Amazonian precipitation decrease and forest dieback under global change warming. *Theoretical and Applied Climatology*, **78**: 157-175.

Bonner WD. 1968. Climatology of the Low-Level Jet. *Montly Weather Review* **96**: 833-850.

Bonner WD, Paegle J. 1970. Diurnal variations in boundary layer winds over the south-central United States in summer. *Montly Weather Review* **98**: 735-744.

Correia FWS, Manzi OA, Candido AL. 2007. Balanço de umidade na Amazônia e sua sensibilidade às mudanças na cobertura vegetal. *Ciencia e Cultura* **59**: 39-43. ISSN 0009-6725.

Chou SC, Bustamante JF, Gomes JL. 2005. Evaluation of Eta model seasonal precipitation forecasts over South America. Nonlinear Processes in Geophysics **12**: 537-555.

Cox PM, Betts RA, Jones CD, Spall SA, Totterdell IJ. 2000. Acceleration of global warming due to carbon-cycle feedbacks in a coupled climate model. *Nature* **408**:184-187.

Douglas MW, Nicolini M, Saulo C. 1998. Observational evidences of a Low-Level Jet east of the Andes during January-March 1998. *Meteorologica* **3**: 63-72.

Christensen et al. 2007. Regional Climate Projections. In: Climate Change 2007: The Physical Science Basis. Chapter 11, Contribution of Working Group I to the Fourth Assessment Report of the Intergovernmental Panel on Climate Change [Solomon, S., D. Qin, M. Manning, Z. Chen, M. Marquis, K.B. Averyt, M. Tignor and H.L. Miller (eds.)]. Cambridge University Press, Cambridge, United Kingdom and New York, NY, USA.

Giorgi F, Mearns LO.1999. Introduction to special section: Regional climate modeling revisited. Journal of Geophysical Research **104**(D6): 6335-6352.

Gordon C, Cooper C, Senior CA, Banks H, Gregory JM, Johns TC, Mitchell JFB, Wood RA. 2000. The simulation of SST, sea ice extent and ocean heat transports in a version of the Hadley Centre coupled model without flux adjustments. *Climate Dynamics* **16**: 147– 168.

Herdies LD, Da Silva A, Dias MAF. 2002. Moisture budget of the bimodal patter of summer circulation over South America. *Journal of Geophysical Research* **107** (D20).

Intergovernmental Panel on Climate Change IPCC (2007a) *Climate Change 2007: The Physical Science Basis Summary for Policymakers Contribution of Working Group I to the Fourth Assessment Report of the Intergovernmental Panel on Climate Change,* 18 pp.

Intergovernmental Panel on Climate Change IPCC (2007b) *Working Group II Contribution to the Intergovernmental Panel on Climate Change Fourth Assessment Report Climate Change 2007: Climate Change Impacts, Adaptation and Vulnerabilit,y* Summary for Policymakers, 23 pp.

Johns TC, Carnell RE, Crossley JF, Gregory JM, Mitchell JFB, Senior CA, Tett SFB, Wood RA. 1997. The Second Hadley Centre coupled ocean-atmosphere GCM: Model description, spinup and validation. *Climate Dynamics* **13**: 103-134.

Jones RG, Noguer M, Hassel DC, Hudson D, Wilson SS, Jenkins GJ, Mitchell JFB. 2004. Generating high resolution climate change scenarios using PRECIS. Meteorological Office Hadley Centre. Exeter, UK, 40.

Jones RG, Murphy JM, Hassell DC, Woodage MJ. 2007. A high resolution atmospheric GCM for the generation of regional climate scenarios. Submitted to *Climate Dynamics*.

Kalnay E, Kanamitsu M, Kistler R, Collins W, Deaven D, Gandin L, Iredell M, Saha S, White G, Woollen J, Zhu Y, Leetmaa A, Reynolds B. 1996. The NCEP/NCAR Reanalysis Project. *Bulletin of the American Meteorological Society* **77**: 437-471.

Li W, Fu R, Dickinson E. 2006. Rainfall and its seasonality over the Amazon in the 21st century as assessed by the coupled models for the IPCC AR4. *Journal of Geophysical Research*, **111**, D02111.

Liebmann B, Kilads GN, Vera CS, Saulo C, Carvalho LMV. 2004. Subseasonal Variations of Rainfall in South America in the Vicinity of the Low-Level Jet East of the Andes and Comparison to Those in the South Atlantic Convergence Zone. . *Journal of Climate* **17:** 3829-3842.

Marengo JA, Ambrizzi T. 2006. Use of regional climate models in impacts assessments and adaptations studies from continental to regional and local scales. **Proccedings of 8 ICSHMO**, INPE: 291-296.

Marengo JA, Soares WR, Nicolini M, Saulo C. 2004. Climatology of Low-Level Jet East of the Andes as derived from the NCEP-NCAR reanalysis: Characteristics and Temporal Variability. *Journal of Climate* **17:** 2261-2280.

Marengo JA, Soares WR. 2002. Episódios de jatos em baixos níveis ao leste dos Andes durante 13-19 de abril de 1999. *Revista Brasileira de Meteorologia* **17**, 35-52.

Marengo JA, Alves L, Valverde M, Rocha R, Laborbe R. 2007. *Eventos extremos em cenários regionalizados de clima no Brasil e América do Sul para o Século XXI: Projeções de clima futuro usando três modelos regionais. Relatório 5*, Ministério do Meio Ambiente - MMA, Secretaria de Biodiversidade e Florestas – SBF, Diretoria de Conservação da Biodiversidade – DCBio Mudanças Climáticas Globais e Efeitos sobre a Biodiversidade, 77p.

Marengo JA, Jones R, Alves L, Valverde MC. 2008. *Future change of temperature and precipitation extremes in South America as derived from the PRECIS regional climate modeling system*, **Submitted**, Int. J. Climatology.

Meehl GA, Washington WM. 1996. El Nino-like climate change in a model with increased atmospheric CO2-concentrations. *Nature*, **382**, 56-60.

Misra V, Dirmeyer P, Kirtman B, Huang H, Kanamitsu M. 2000. Regional simulation of Interannual Variability over South América. *COLA Technical Report*. USA, 85.

Nakicenovic N, Alcamo J, Davis G, de Vries B, Fenhann J, Gaffin S, Gregory K, Grubler A, Jung TY, Kram T, La Rovere EL, Michaelis L, Mori S, Morita T, Pepper W, Pitcher H, Price L, Riahi K, Roehrl A, Rogner H-H, Sankovski A, Schlesinger M, Shukla P, Smith S, Swart R, van Rooijen S, Victor N, Dadi Z (2000) Special report on emissions scenarios Cambridge 599pp

Nicolini MP, Salio JJ, Katzfey J, McGregor L, Saulo AC. 2002. January and July regional climate simulation over South American. *Journal of Geophysical Research* **107**, NO. D22, 4637.

Nicolini M, Saulo C. 2006. Modeled Chaco low-level jets and related precipitation atterns during the 1997–1998 warm season. *Meteorology and Atmospheric Physics* **94**: 129–143. DOI 10.1007/s00703-006-0186-7.

Nogués-Paegle JN, MO KC. 1997. Alternating wet and dry conditions over south america during summer. *Montly Weather Review* **125**: 279–291.

Paegle JA. 1998. A comparative review of South American low-level jets. *Meteorologica* **3**, 73-82.

Pope VD, Gallani ML, Rowntree PR, Stratton RA. 2000. The impact of new physical parametrizations in the Hadley Centre climate model - HadAM3. *Climate Dynamics* **16**: 123-146.

Rao VB, Chapa SR, Franchito SH. 1999. Decadal variation of atmosphere-ocean interastion in the tropical Atlantic and its relationship to the Northeast-Brazil rainfall. *Journal of the Meteorological Society of Japan* **77**: 63-75.

Rayner NA, Parker DE, Horton EB, Folland CK, Alexander LV, Rowell DP, Kent EC, Kaplan A.2003. Global analyses of sea surface temperature, sea ice, and night marine air temperature since the late nineteenth century, *Journal of Geophysical Research* **108** (D14): 4407, DOI 10.1029/2002JD002670.

Robock A, Scholosser C A, Vinnikov KY.; Speranskaya NA.; Entin JK, Qui S. 1998. Evaluation of the AMIP soil moisture simulations. Global and Planetary Change**19**: 181-202.

Rowell DP. 2005. A scenario of European climate change for the late twenty-first century: Seasonal means and interannual variability. *Climate Dynamics* **25**: 837– 849, doi:10.1007/s00382-005-0068-6.

Salazar L, Nobre C, Oyama M. 2007. Climate change consequences on the biome distribution in tropical South America. *Geophysical Research Letters* **34**. L09708, doi:10.1029/2007GL029695.

Salio P, Nicolini, M, Saulo C. 2002. Chaco low-level jet events characterization during the austral summer season. *Journal of Geophysical Research* **107**: D24, 4816 10.1029/2001JD001315. 34.

Salio P, Nicolini, M, ZIPSER EJ. 2007. Mesoscale Convective Systems over Southeastern South America and Their Relationship with the South American Low-Level Jet *Montly Weather Review* **135**: 1290-1309, DOI: 10.1175/MWR3305.1

Saulo C, Nicolini M, Chou SC. 2000. Model characterization of the South American low-level flow during the 1997-98 spring-summer season. *Climate Dynamics* **16**: 867-881.

Saulo C, Ruiz J, Skabar YG. 2007. Synergism between the Low-Level Jet and Organized Convection at Its Exit Region. *Montly Weather Review* **135**: 1310–1326. DOI: 10.1175/MWR3317.1.

Sampaio G, Nobre C, Costa HM, Satyamurty P, Soares-Filho BS, Cardoso M. 2007. Regional climate change over eastern Amazonia caused by pasture and soybean cropland expansion. *Geophysical Research Letters* **34**: L17709, doi:10.1029/2007GL030612.

Vera CS, and Coauthors, 2006a. The South American Low-Level Jet Experiment. *Bulletin of the American Meteorological Society* **87:** 63–77.

Vera CS, Silvestri G, Liebmann B, González P. 2006b. Climate change scenarios for seasonal precipitation in South America from IPCC-AR4 models. *Geophysical Research Letters* **33**, L13707, doi:10.1029/2006GL025759.

Vera CS, and Coauthors 2006c: Toward a Unified View of the American Monsoon Systems 4977-5000., *Journal of Climate* **19**: WN: 0628807462003.

Vernekar AD, Kirtman BP, Fennessy MJ. 2003. Low-Level Jets and their effects on the South America summer climate as simulated by the NCEP Eta/CPTEC model. *Journal of Climate* **16**: 297-311.

Whiteman C, Bian X, Zhong S. 1997. Low-level jet climatology from enhanced rawinsonde observations at a site in the southern Great Plains. *Journal of Applied Meteorology* **36:** 1363–1375.

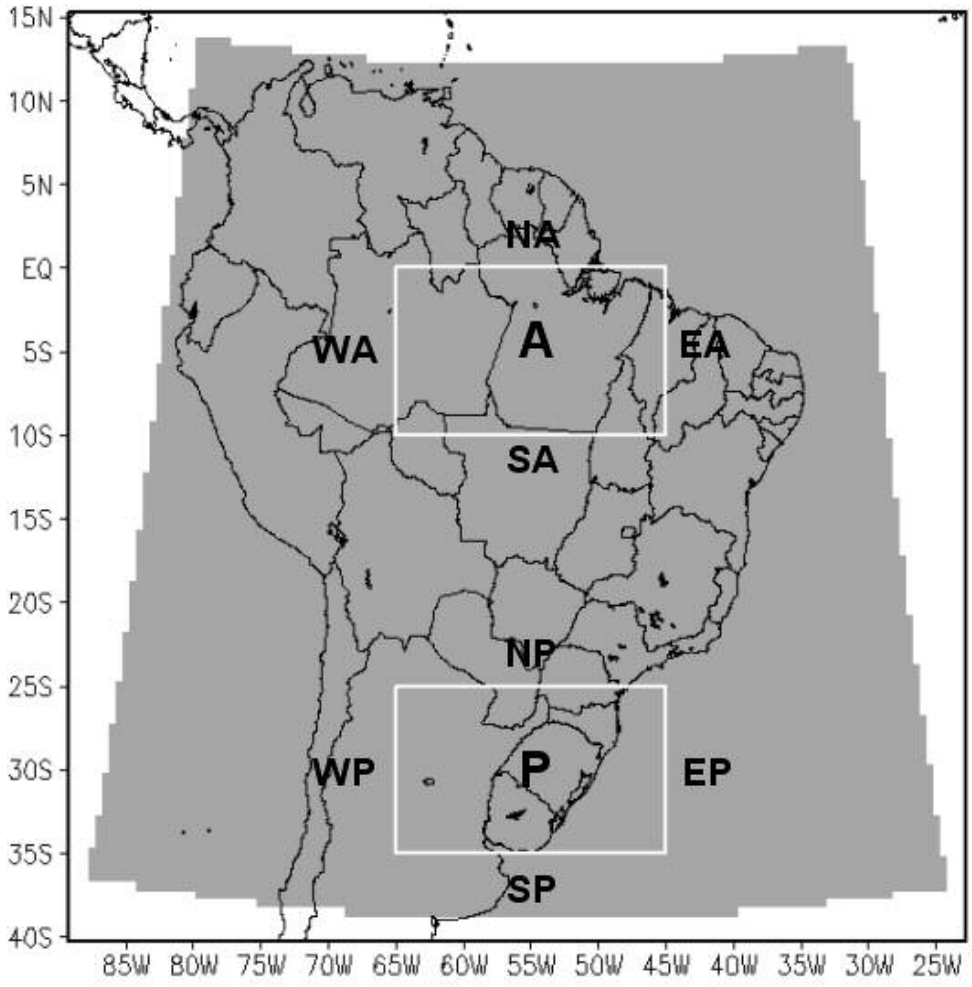

Figure 1. Areas under study shown in the regional model. The rectangles mark the regions of the Amazon (A) and La Plata basins (P).
141x143mm (96 x 96 DPI)

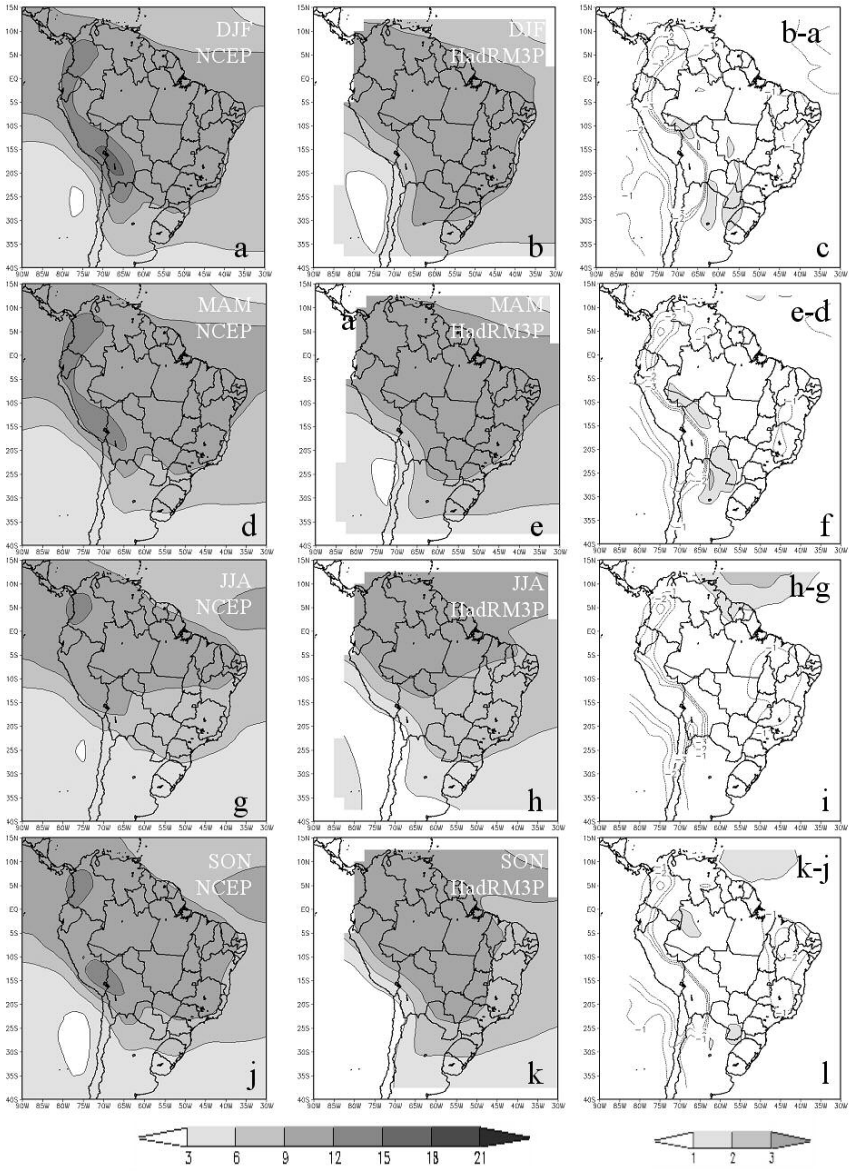

Figure 2. Specific humidity (g.kg-1) between the surface and 700hPa. Figures a (DJF), d (MAM), g (JJA) and j (SON) were obtained from NCEP reanalyses for the 1980 to 1989 period. Figures b (DJF), e (MAM), h (JJA) and k (SON) were obtained from HadRM3P for same period. The Figures c, f, i e l are the difference fields between b-a, e-d, g- h, e k-j respectively. Units are g kg-1.
247x340mm (96 x 96 DPI)

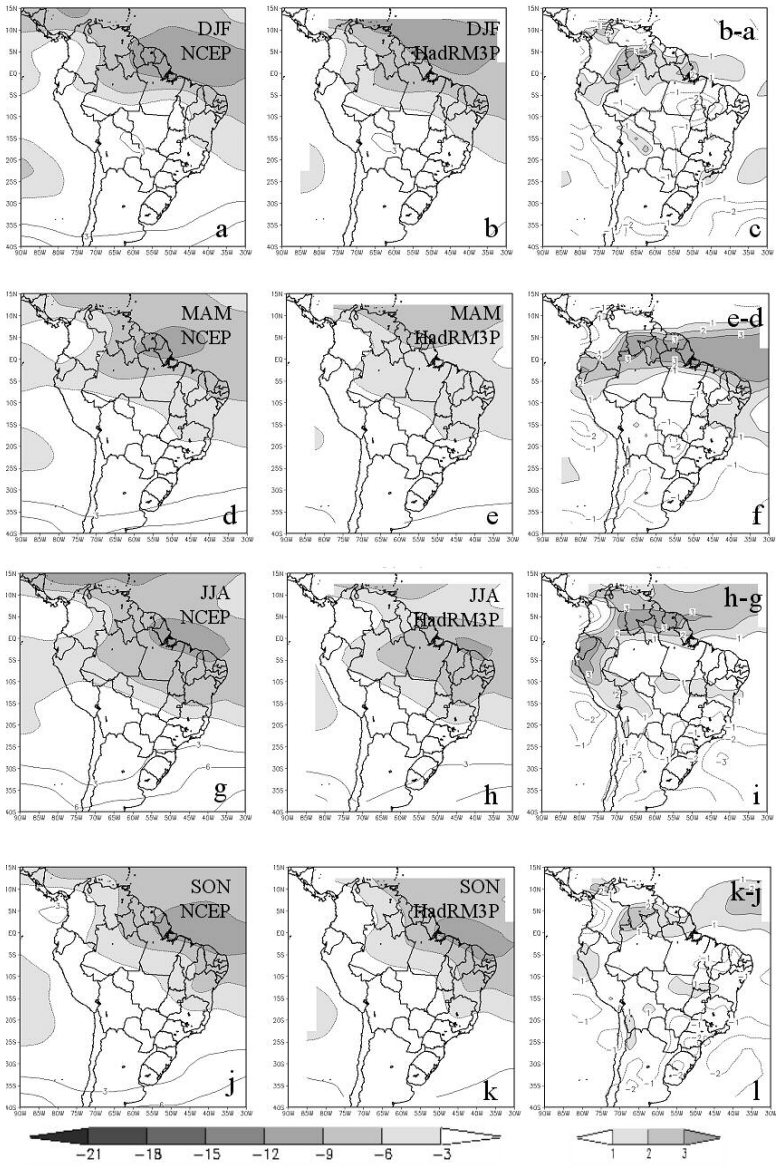

Figure 3. Fields of zonal wind below 700 hPa. Figures a (DJF), d (MAM), g (JJA) and j (SON)) were obtained from NCEP reanalyses for the 1980 to 1989 period. Figures b (DJF), e (MAM), h (JJA) and k (SON) were obtained from HadRM3P for same period. Figures c, f, i e l are the difference fields between b-a, e-d, g- h, e k-j respectively. Units are m s-1.

224x341mm (96 x 96 DPI)

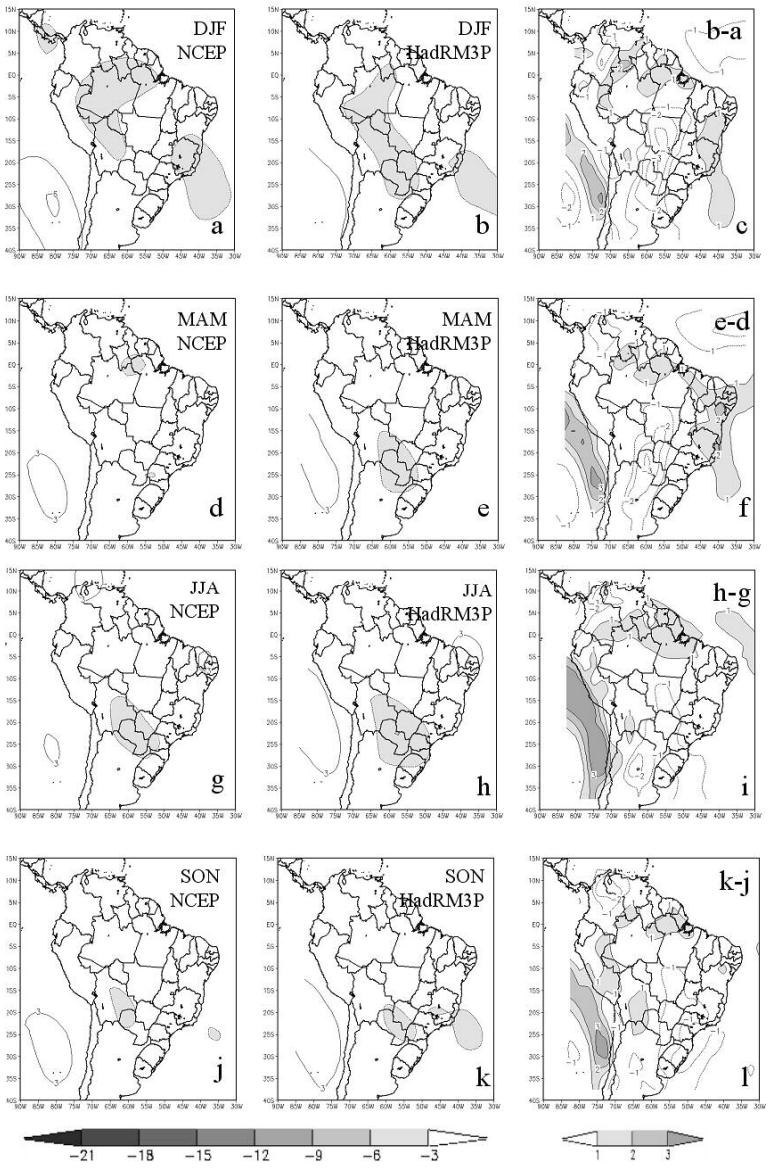

Figure 4. Same as in Figure 3, but for meridional wind component.
225x347mm (96 x 96 DPI)

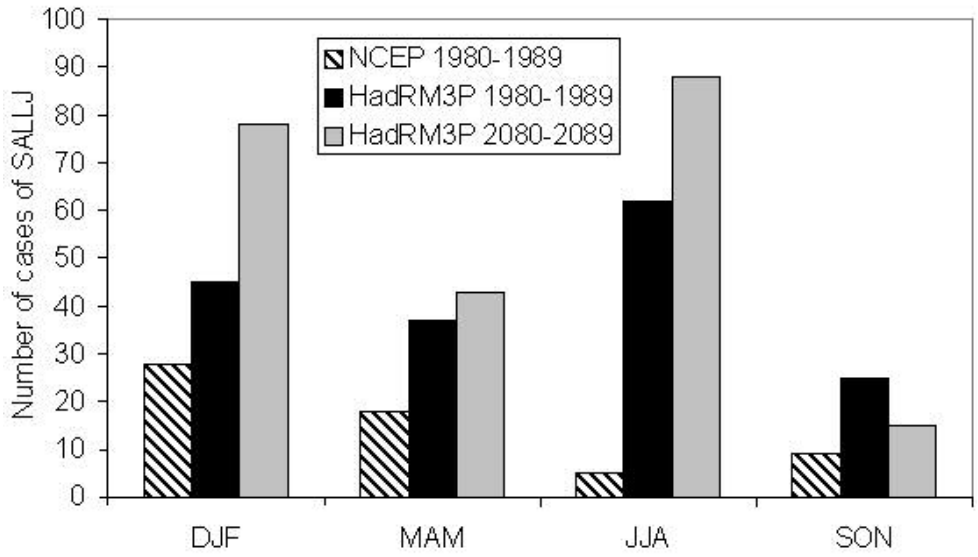

Figure 5. Number of detected SALLJs in Santa Cruz de la Sierra in Bolivia (17.7S, 63W) using the modified Bonner criteria 1.
146x86mm (96 x 96 DPI)

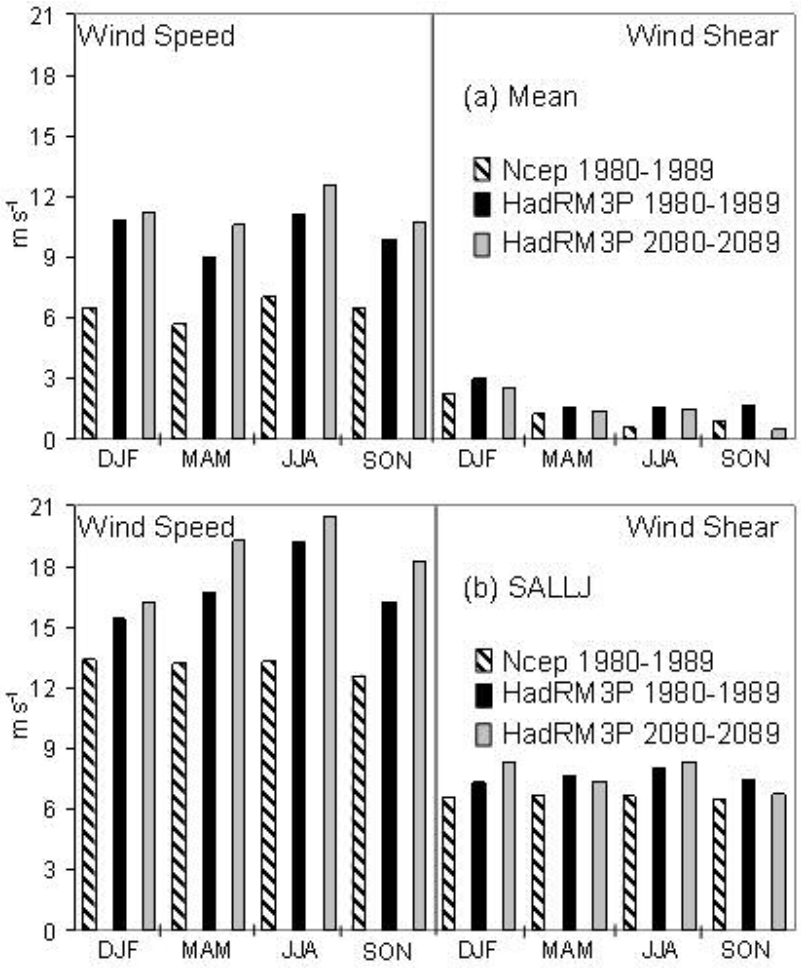

Figure 6. Magnitude of the wind at 850hPa and vertical wind shear between the 850 and 700 hPa levels. a) Average, b) Composite of SALLJ events. Units are m s-1.
110x131mm (96 x 96 DPI)

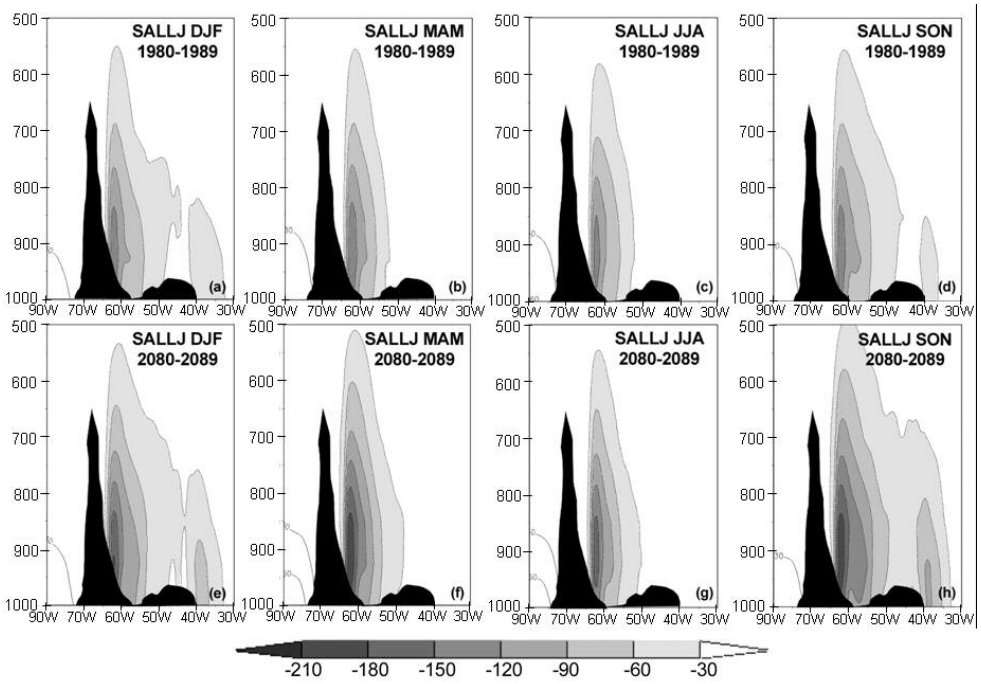

Figure 7. Vertical cross section of the meridional moisture transport along the latitude of Santa Cruz de la Sierra in Bolivia (17.7S). Units are m g s-1 kg-1.
243x180mm (96 x 96 DPI)

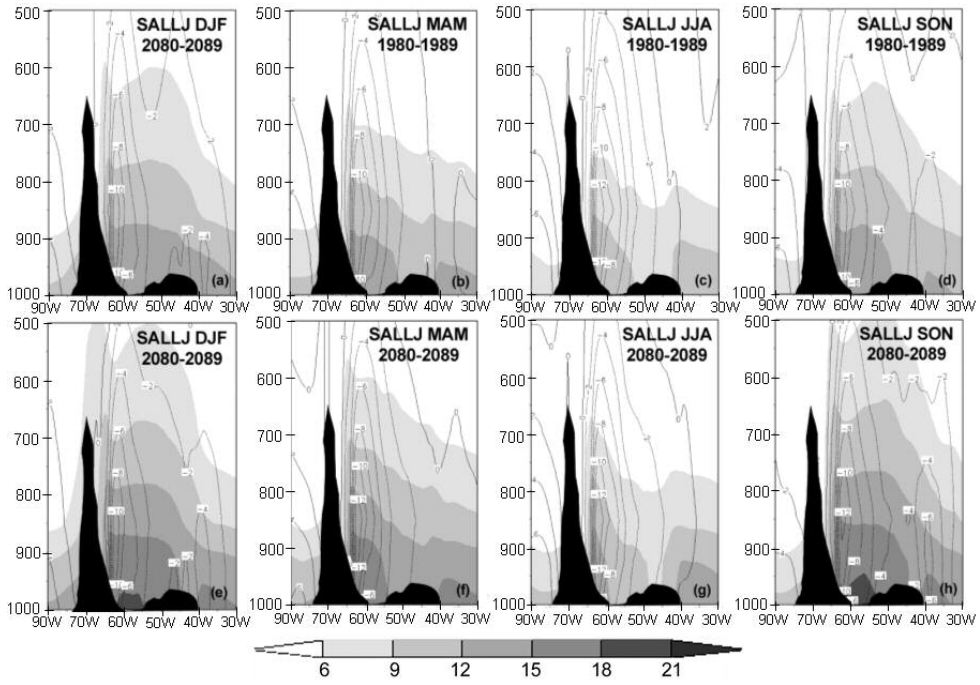

Figure 8. Vertical cross section of the meridional component of the wind (m.s-1) and specific humidity (g kg-1) along the latitude of Santa Cruz de la Sierra in Bolivia (17.7S).
240x169mm (96 x 96 DPI)

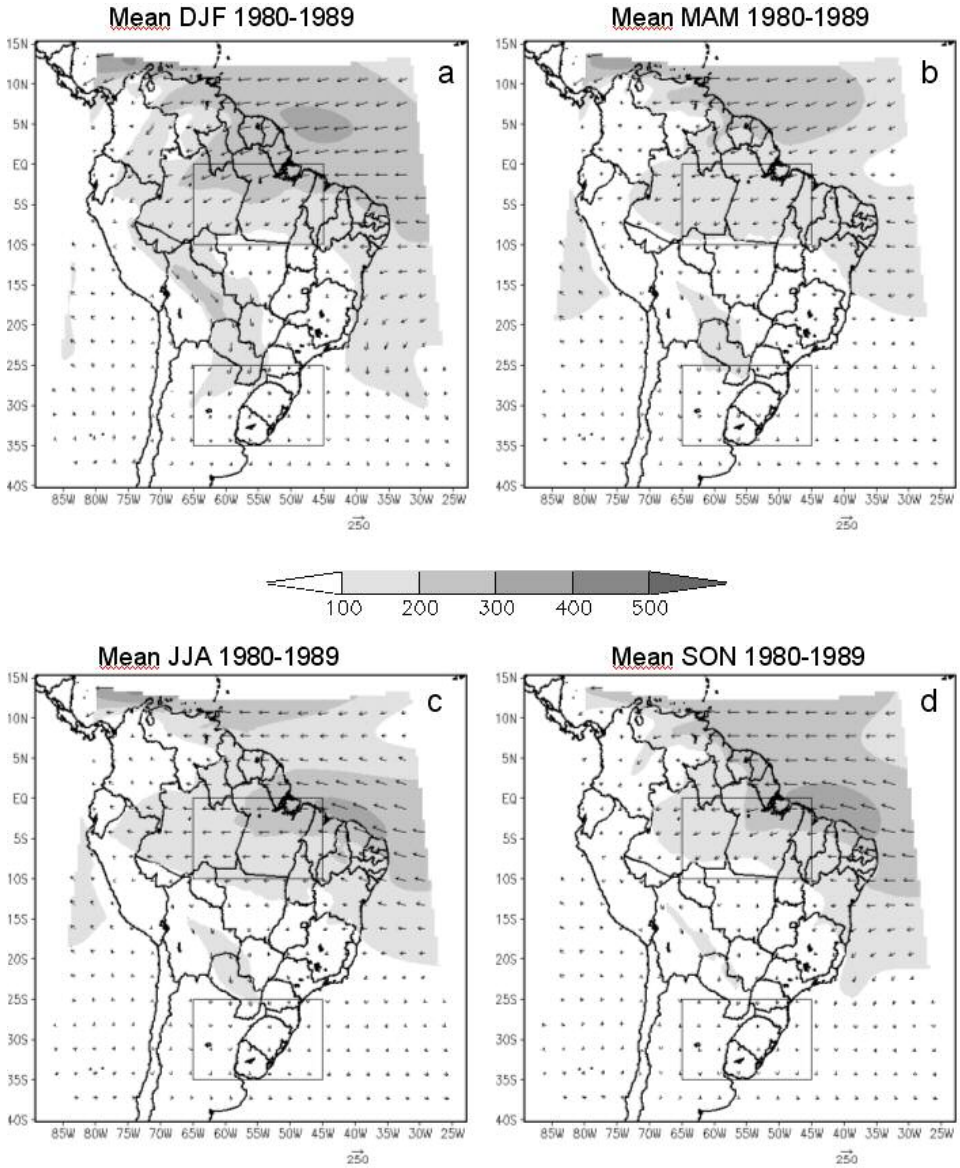

Figure 9. Fields of vertically integrated moisture flux between the surface and 700hPa. a ,b, c and d representing the average fields during 1980-1989 for the trimesters DJF, MAM, JJA and SON respectively. Figures e, f, g and h are for 2080-2089. i, j, k and l represent composites of SALLJ in the period 1980-1989 for the trimesters DJF, MAM, JJA and SON respectively. m, n, o and p represent composites of SALLJ for 2080-2089 respectively. Units are kg (m s)-1.
189x226mm (96 x 96 DPI)

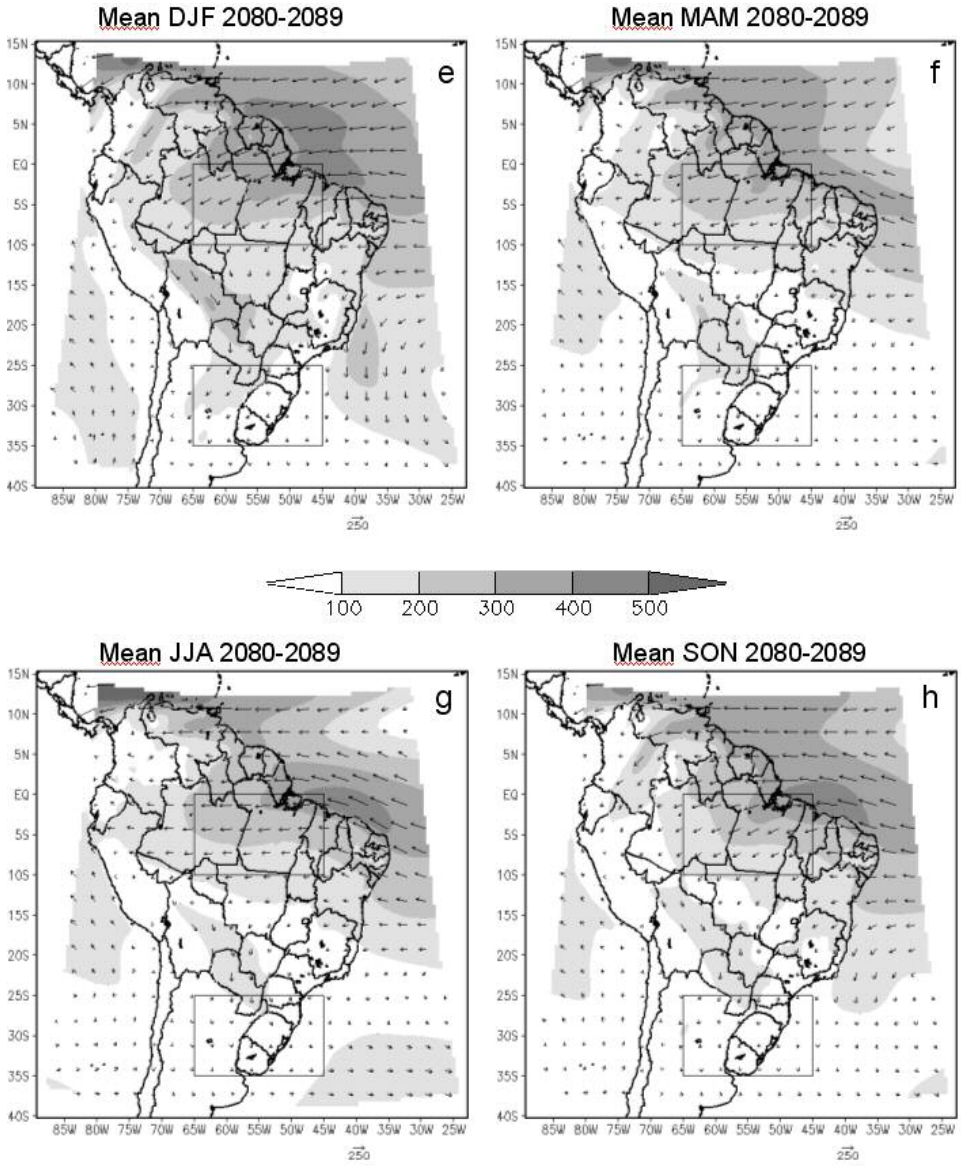

Figure 9. Continuated.
186x227mm (96 x 96 DPI)

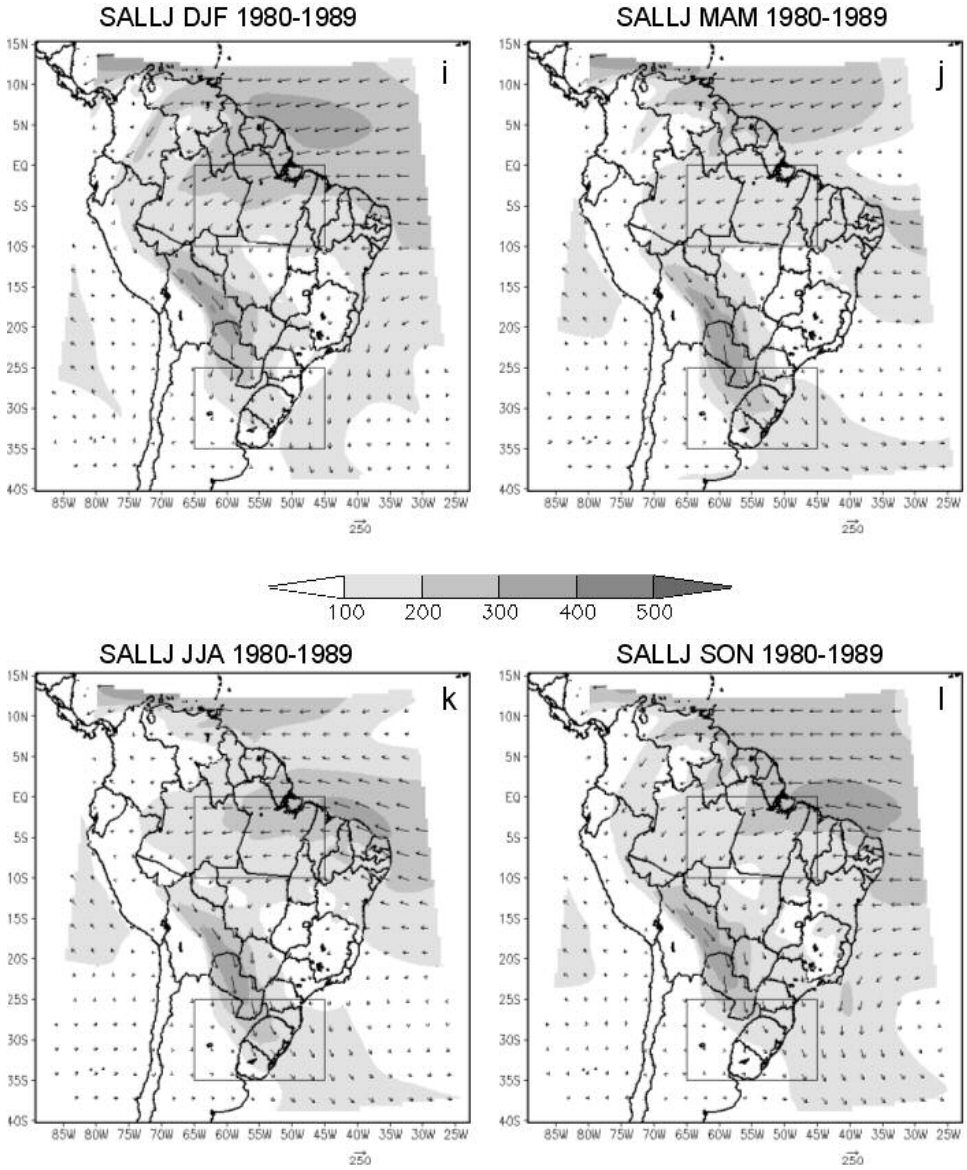

Figure 9. Continuated.
188x225mm (96 x 96 DPI)

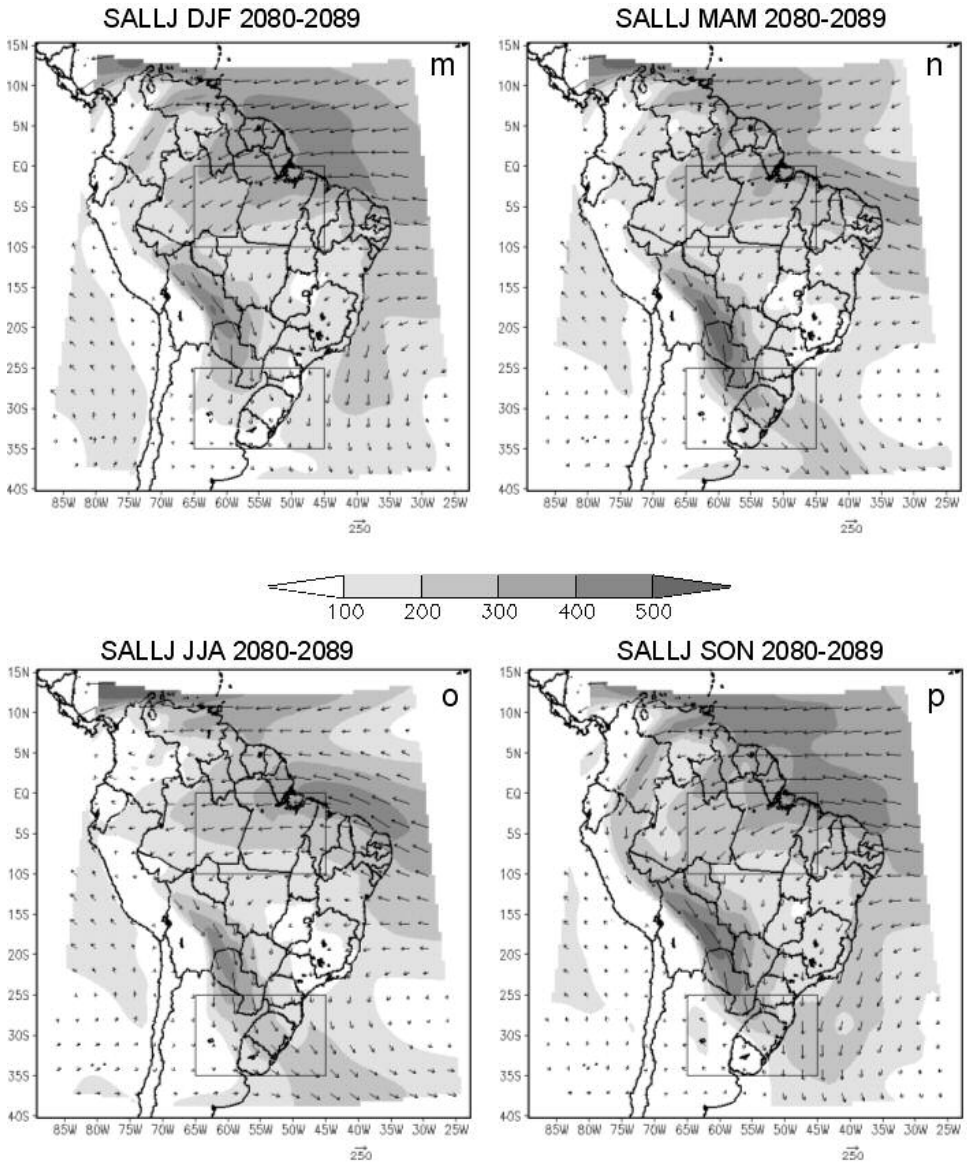

Figure 9. Continuated.
188x224mm (96 x 96 DPI)

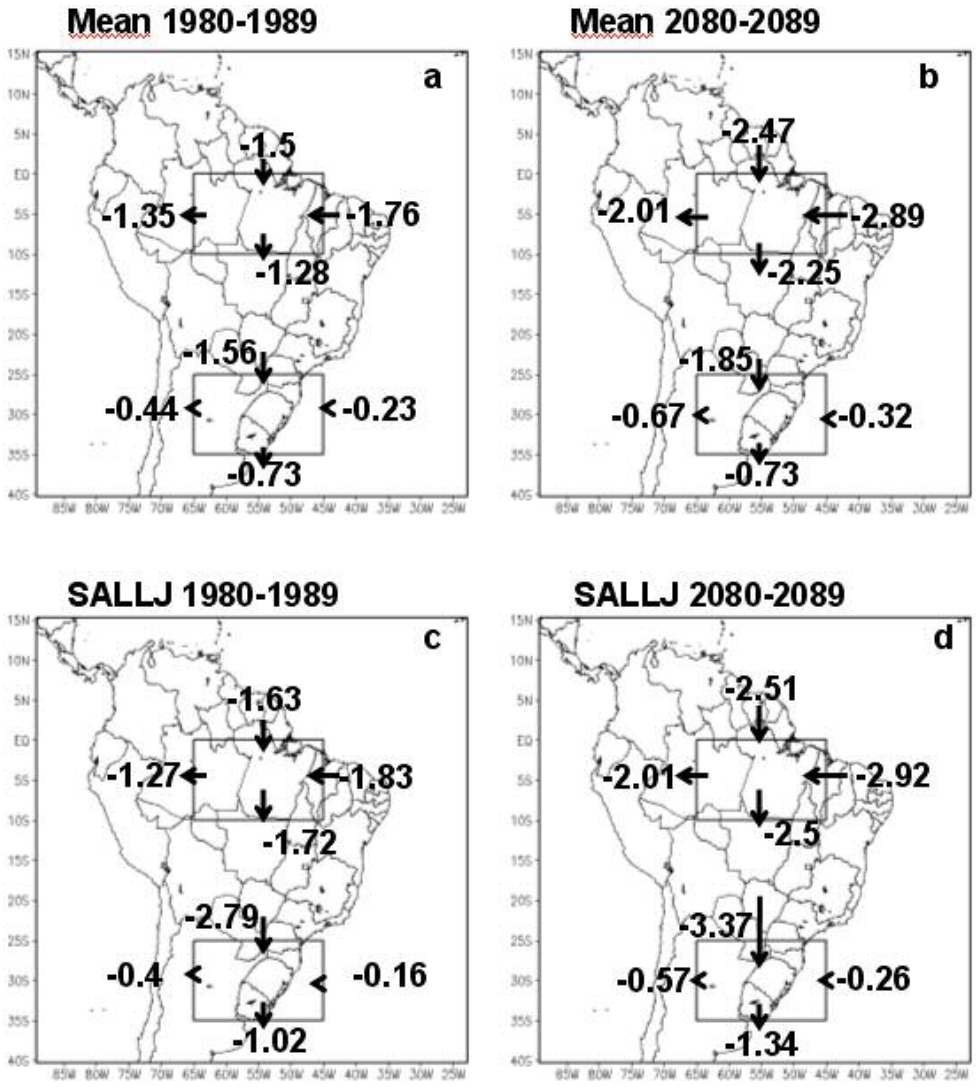

Figure 10. Components of the moisture flow integrated along the lateral boundaries of representative areas of the Amazon and La Plata basin during DJF. The numbers in the center of the rectangles represent the horizontal moisture divergence. Units are x108kg s-1.

145x161mm (96 x 96 DPI)

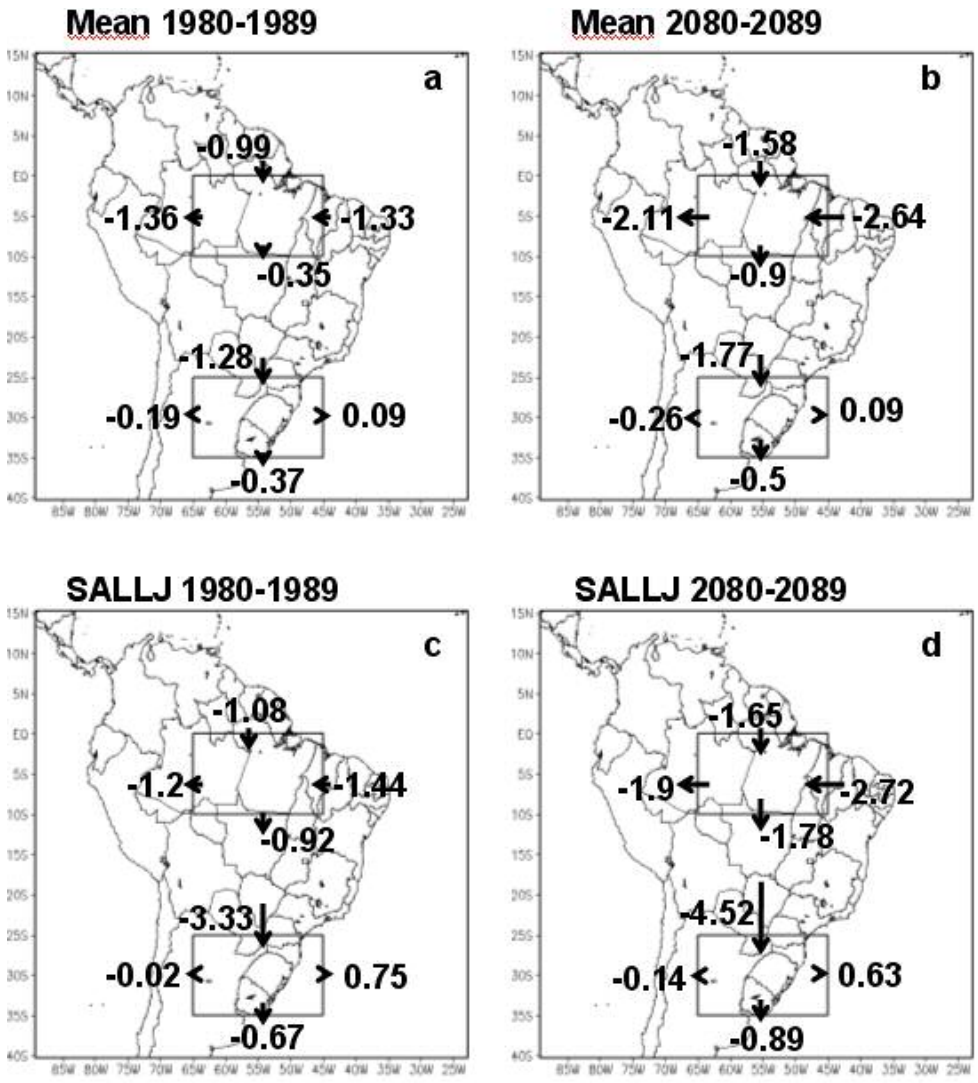

Figure 11. Same as in figure 7, but for MAM.
144x160mm (96 x 96 DPI)

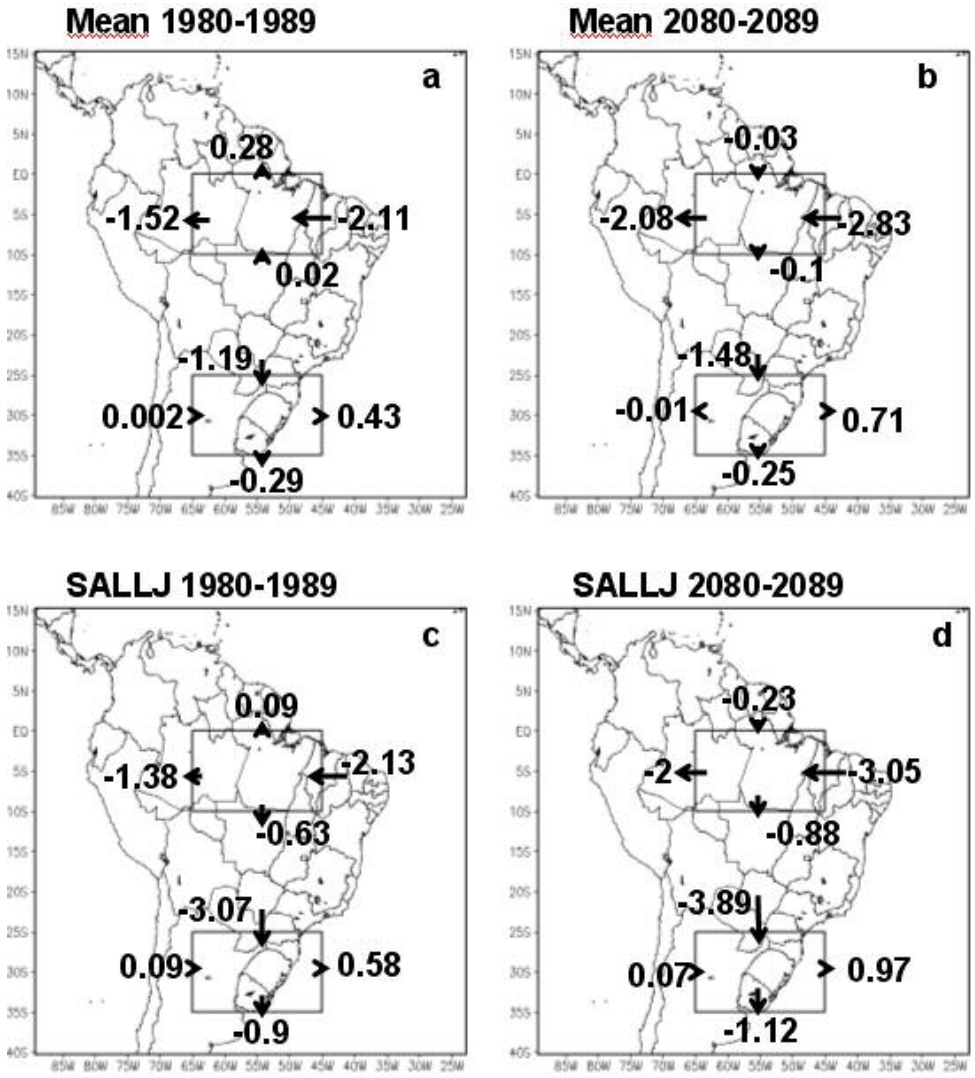

Figure 12. Same as in figure 7, but for JJA.
145x161mm (96 x 96 DPI)

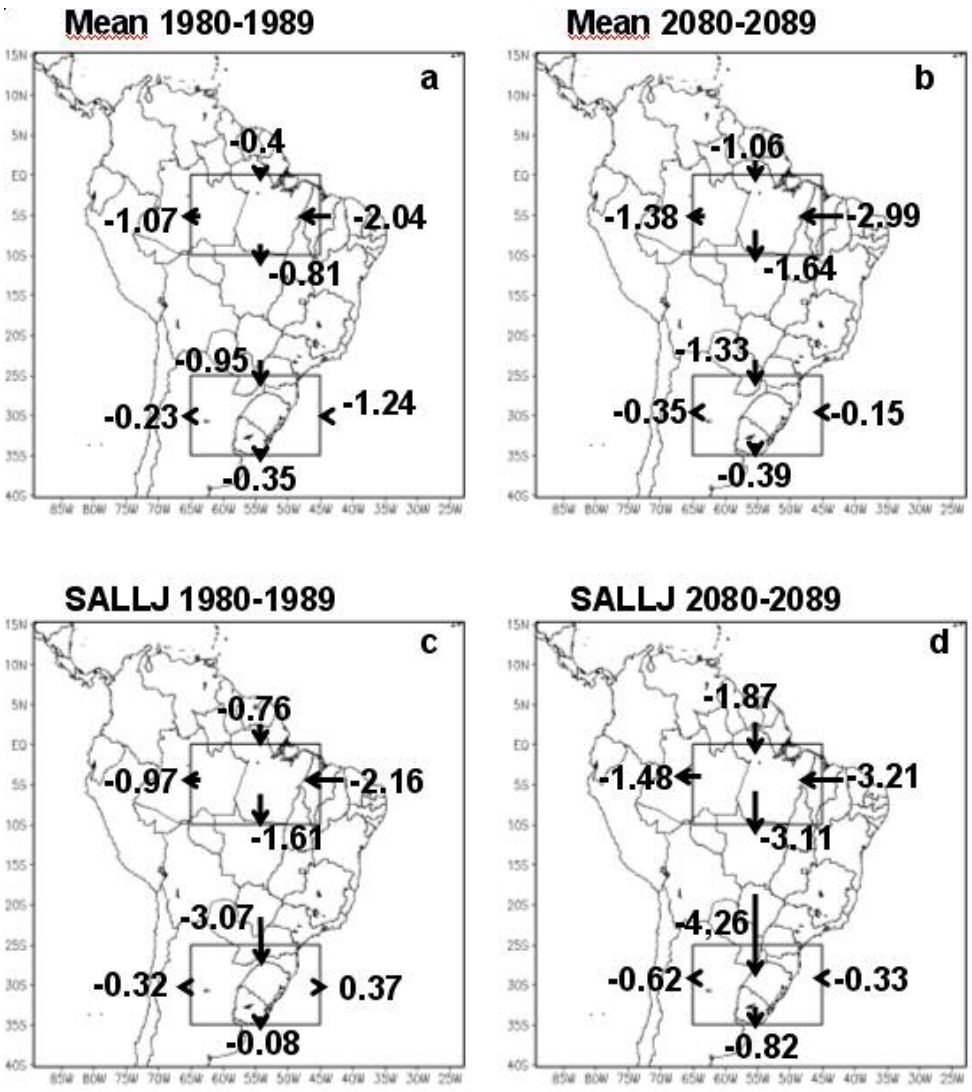

Figure 13. Same as in figure 7, but for SON.
145x162mm (96 x 96 DPI)

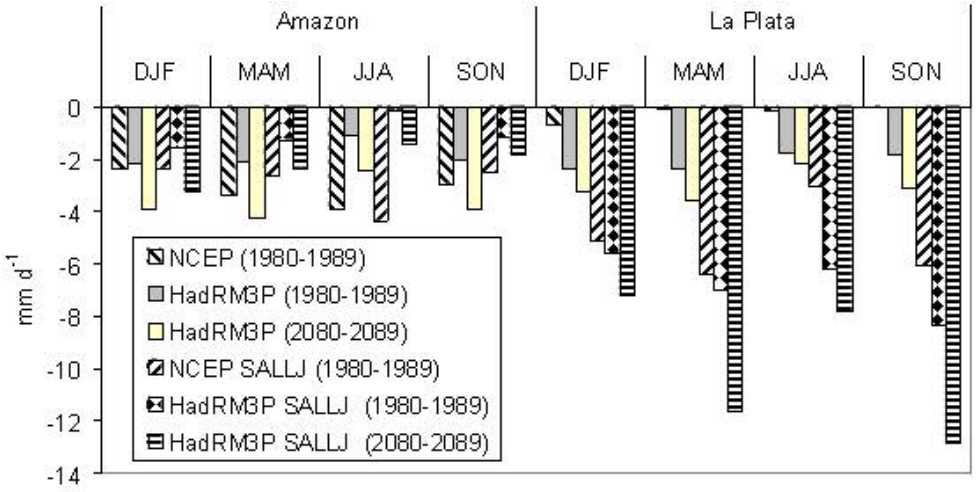

Figure 14. Moisture divergence in the Amazon and La Plata basins. Negative values of divergence indicate convergence. Units are mm d-1.
146x74mm (96 x 96 DPI)

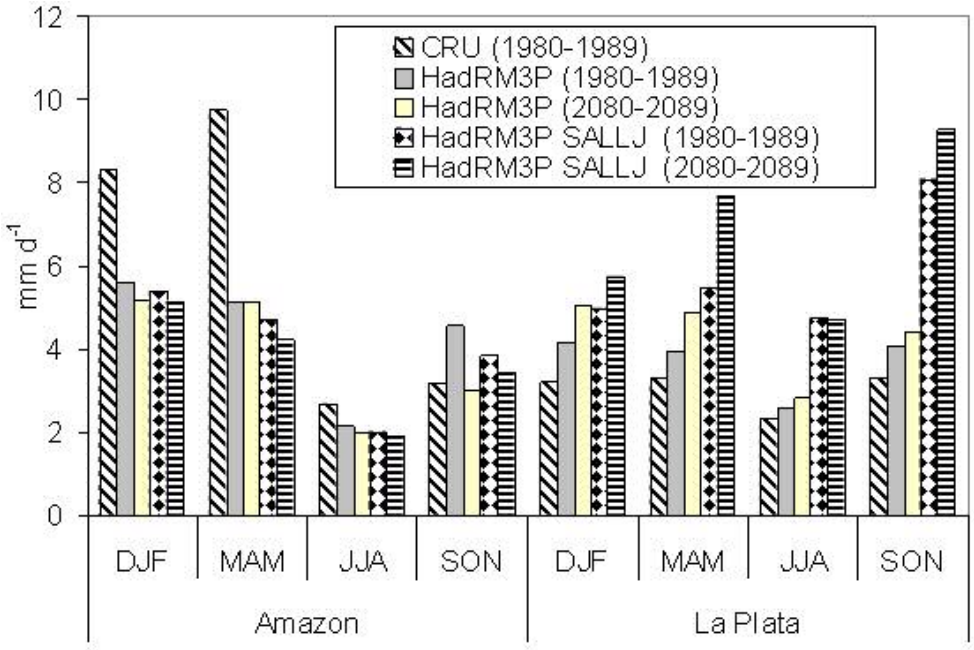

Figure 15. Precipitation in the Amazon and La Plata basins. Units are mm d-1.
146x97mm (96 x 96 DPI)